with CAMPATH-1H also resulted in a significant increase in cell death in primary cells from three patients with EVI1^{High} AML (PT8, PT9 and PT11), and no response was observed in the case of the EVI1^{Low} PT1 cells (Figure 4b, right panel). These results suggest that CAMPATH-1H exerts a significantly stronger ADCC effect than a CDC effect against EVI1^{High} AML.

In vivo *antitumor effect of CAMPATH against EVI1^{High} AML in a xenograft model*

To investigate the effects of CAMPATH-1H on EVI1^{High} AML *in vivo*, USCD/AML1 cells with EVI1^{High} expression were subcutaneously inoculated into immunodeficient NOG mice. After tumors reached a size of 50–100 mm^3, 100 μg of CAMPATH-1H or PBS as a control was intravenously injected once a week for 4 weeks, and tumor growth and mouse survival were monitored (Figures 4c and d). CAMPATH-1H significantly inhibited the tumor growth of UCSD/AML1 cells when compared with the control ($P<0.05$) (Figure 4c). The median survival time of control mice was 75 days, and all control mice died within 100 days. In contrast, the median survival was prolonged to 127 days in mice injected with CAMPATH-1H, and four out of five mice were still alive more than 100 days after inoculation. Taken together, these data suggest that CAMPATH-1H is a promising candidate therapeutic antibody for AML patients with EVI1^{High} expression.

Discussion

In this study, we found that CD52 was highly expressed in most EVI1^{High} leukemia cells. Using the humanized anti-CD52 monoclonal antibody CAMPATH-1H, we showed that CAMPATH-1H inhibited cell growth and induced apoptosis of EVI1^{High} leukemia cells through direct cytotoxicity and/or ADCC *in vitro*. Moreover, we showed the therapeutic efficacy of CAMPATH-1H in an *in vivo* model of EVI1^{High} leukemia using NOG mice. Although NOG mice lack functional T and natural killer cells, murine neutrophils were considered to be effector cells mediating ADCC as well as direct cytotoxicity in our mouse model. Indeed, CAMPATH-1H efficiently inhibited the growth of leukemia xenografts in an EVI1^{High} AML xenograft model. These data suggest that the use of CAMPATH-1H may be effective in treating myeloid leukemia with EVI1^{High}.

CD52 is a small glycosylphosphatidylinositol-linked protein of unknown function. CAMPATH-1H (Alemtuzumab), a humanized antibody against CD52, is used to deplete leukemia cells from patients with relapsed/refractory chronic lymphocytic leukemia.[15] Recent studies have suggested the effectiveness of CAMPATH-1H treatment in additional hematopoietic malignancies, including peripheral T-cell lymphoma, T-cell prolymphocytic leukemia and cutaneous T-cell lymphoma.[40–42] Although it has been reported that the majority of various subtypes of AML are negative for CD52 expression, a subset of acute myelomonocytic leukemias has been shown to exhibit CD52 expression.[13] This is consistent with our observation that a case (no. 2) out of 10 EVI1^{Low} AML cases has been diagnosed with myelomonocytic leukemia with high CD52 expression (Supplementary Figure S1). Recently, it was reported that 15 patients with CD52-positive, recurrent or refractory acute leukemia (nine patients with AML and six patients with ALL) received single-agent Alemtuzumab.[14] Interestingly, the majority of the CD52-positive AML cases had chromosome 7 abnormalities, and two cases with monosomy 7 exhibited complete remission. In our study, five of nine AML patients with EVI1^{High} expression displayed chromosomal abnormalities involving chromosome 7, such as t(3;7)(q26;q21), partial deletion of chromosome 7 or monosomy 7. Patients with EVI1^{High} AML exhibit specific clinical features, including elevated platelet counts, association with monosomy 7 or chromosome 7 deletion, refractoriness to therapy and a poor prognosis.[43] It has been suggested that the genomic instability and myelodysplasia with monosomy 7 occur as a consequence of EVI1 activation after gene therapy for chronic granulomatous disease.[44] It seems likely that EVI1 and gene(s) on chromosome 7 play a crucial role in regulating CD52 expression. We have previously shown that EVI1 is expressed on bone marrow stem and progenitor cells and has an important function in maintaining hematopoietic stem cells.[45] It is, therefore, tempting to speculate that specific stem cell populations may express CD52 along with EVI1. Future studies should examine the expression of CD52 on hematopoietic stem cells and its relevance to leukemia development. It is also important to determine whether EVI1 directly activates the CD52 promoter.

Although the mechanism of cytotoxicity of CAMPATH-1H is not well understood, CAMPATH-1H had minimal direct cytotoxicity, but exhibited significant CDC against chronic lymphocytic leukemia and acute lymphocytic leukemia cells.[18,19] In our experiments, CAMPATH-1H lysed EVI1^{High} AML cells more efficiently through direct cytotoxicity or ADCC than through CDC (Figures 3 and 4). CD52 is a 12-amino-acid glycopolypeptide containing a large glucose moiety, and CAMPATH-1H recognizes C-terminal amino acids and part of the glycosylphosphatidylinositol anchor of CD52.[46,47] The amount of protein and/or post-translational modifications, such as glycosylation, may be involved in differential immune responses to CAMPATH-1H.

We showed that EVI1^{High} AML cells are good targets for the cytolytic activity of CAMPATH-1H. In the standard schedule of CAMPATH-1H for allogeneic stem cell transplantation, the treatment is not always efficient because the antibody adsorbs onto T lymphocytes. Therefore, combinations of CAMPATH-1H with active chemotherapeutic agents such as daunorubicin, etoposide and cytarabine need to be explored in future studies. Finally, these studies provide support for a clinical trial of CAMPATH-1H in patients with EVI1^{High} AML and potentially in patients with other AMLs that express CD52.

Conflict of interest

The authors declare no conflict of interest.

Acknowledgements

We gratefully acknowledge Genzyme for providing the CAMPATH-1H antibody for the study.

References

1 Morishita K, Parker DS, Mucenski ML, Jenkins NA, Copeland NG, Ihle JN. Retroviral activation of a novel gene encoding a zinc finger protein in IL-3-dependent myeloid leukemia cell lines. *Cell* 1988; **54**: 831–840.
2 Mucenski ML, Taylor BA, Ihle JN, Hartley JW, Morse III HC, Jenkins NA *et al.* Identification of a common ecotropic viral integration site, Evi-1, in the DNA of AKXD murine myeloid tumors. *Mol Cell Biol* 1988; **8**: 301–308.
3 Morishita K, Parganas E, William CL, Whittaker MH, Drabkin H, Oval J *et al.* Activation of EVI1 gene expression in human acute myelogenous leukemias by translocations spanning 300–400

kilobases on chromosome band 3q26. *Proc Natl Acad Sci USA* 1992; **89**: 3937–3941.
4 Mitani K, Ogawa S, Tanaka T, Miyoshi H, Kurokawa M, Mano H *et al.* Generation of the AML1-EVI-1 fusion gene in the t(3;21)(q26;q22) causes blastic crisis in chronic myelocytic leukemia. *EMBO J* 1994; **13**: 504–510.
5 Lugthart S, Groschel S, Beverloo HB, Kayser S, Valk PJ, van Zelderen-Bhola SL *et al.* Clinical, molecular, and prognostic significance of WHO type inv(3)(q21q26.2)/t(3;3)(q21;q26.2) and various other 3q abnormalities in acute myeloid leukemia. *J Clin Oncol* 2010; **28**: 3890–3898.
6 Barjesteh van Waalwijk van Doorn-Khosrovani S, Erpelinck C, van Putten WL, Valk PJ, van der Poel-van de Luytgaarde S, Hack R *et al.* High EVI1 expression predicts poor survival in acute myeloid leukemia: a study of 319 *de novo* AML patients. *Blood* 2003; **101**: 837–845.
7 Lugthart S, van Drunen E, van Norden Y, van Hoven A, Erpelinck CA, Valk PJ *et al.* High EVI1 levels predict adverse outcome in acute myeloid leukemia: prevalence of EVI1 overexpression and chromosome 3q26 abnormalities underestimated. *Blood* 2008; **111**: 4329–4337.
8 Groschel S, Lugthart S, Schlenk RF, Valk PJ, Eiwen K, Goudswaard C *et al.* High EVI1 expression predicts outcome in younger adult patients with acute myeloid leukemia and is associated with distinct cytogenetic abnormalities. *J Clin Oncol* 2010; **28**: 2101–2107.
9 Xia MQ, Tone M, Packman L, Hale G, Waldmann H. Characterization of the CAMPATH-1 (CDw52) antigen: biochemical analysis and cDNA cloning reveal an unusually small peptide backbone. *Eur J Immunol* 1991; **21**: 1677–1684.
10 Valentin H, Gelin C, Coulombel L, Zoccola D, Morizet J, Bernard A. The distribution of the CDW52 molecule on blood cells and characterization of its involvement in T cell activation. *Transplantation* 1992; **54**: 97–104.
11 Xia MQ, Hale G, Lifely MR, Ferguson MA, Campbell D, Packman L *et al.* Structure of the CAMPATH-1 antigen, a glycosylphosphatidylinositol-anchored glycoprotein which is an exceptionally good target for complement lysis. *Biochem J* 1993; **293**: 633–640.
12 Osterborg A, Dyer MJ, Bunjes D, Pangalis GA, Bastion Y, Catovsky D *et al.* Phase II multicenter study of human CD52 antibody in previously treated chronic lymphocytic leukemia. European Study Group of CAMPATH-1H Treatment in Chronic Lymphocytic Leukemia. *J Clin Oncol* 1997; **15**: 1567–1574.
13 Rodig SJ, Abramson JS, Pinkus GS, Treon SP, Dorfman DM, Dong HY *et al.* Heterogeneous CD52 expression among hematologic neoplasms: implications for the use of alemtuzumab (CAMPATH-1H). *Clin Cancer Res* 2006; **12**: 7174–7179.
14 Tibes R, Keating MJ, Ferrajoli A, Wierda W, Ravandi F, Garcia-Manero G *et al.* Activity of alemtuzumab in patients with CD52-positive acute leukemia. *Cancer* 2006; **106**: 2645–2651.
15 Alinari L, Lapalombella R, Andritsos L, Baiocchi RA, Lin TS, Byrd JC. Alemtuzumab (Campath-1H) in the treatment of chronic lymphocytic leukemia. *Oncogene* 2007; **26**: 3644–3653.
16 Hale C, Bartholomew M, Taylor V, Stables J, Topley P, Tite J. Recognition of CD52 allelic gene products by CAMPATH-1H antibodies. *Immunology* 1996; **88**: 183–190.
17 Hale G. The CD52 antigen and development of the CAMPATH antibodies. *Cytotherapy* 2001; **3**: 137–143.
18 Zent CS, Chen JB, Kurten RC, Kaushal GP, Lacy HM, Schichman SA. Alemtuzumab (CAMPATH 1H) does not kill chronic lymphocytic leukemia cells in serum free medium. *Leuk Res* 2004; **28**: 495–507.
19 Golay J, Cortiana C, Manganini M, Cazzaniga G, Salvi A, Spinelli O *et al.* The sensitivity of acute lymphoblastic leukemia cells carrying the t(12;21) translocation to campath-1H-mediated cell lysis. *Haematologica* 2006; **91**: 322–330.
20 Greenwood J, Clark M, Waldmann H. Structural motifs involved in human IgG antibody effector functions. *Eur J Immunol* 1993; **23**: 1098–1104.
21 Zhang Z, Zhang M, Goldman CK, Ravetch JV, Waldmann TA. Effective therapy for a murine model of adult T-cell leukemia with the humanized anti-CD52 monoclonal antibody, Campath-1H. *Cancer Res* 2003; **63**: 6453–6457.
22 Golay J, Manganini M, Rambaldi A, Introna M. Effect of alemtuzumab on neoplastic B cells. *Haematologica* 2004; **89**: 1476–1483.
23 Stanglmaier M, Reis S, Hallek M. Rituximab and alemtuzumab induce a nonclassic, caspase-independent apoptotic pathway in B-lymphoid cell lines and in chronic lymphocytic leukemia cells. *Ann Hematol* 2004; **83**: 634–645.
24 Mone AP, Cheney C, Banks AL, Tridandapani S, Mehter N, Guster S *et al.* Alemtuzumab induces caspase-independent cell death in human chronic lymphocytic leukemia cells through a lipid raft-dependent mechanism. *Leukemia* 2006; **20**: 272–279.
25 Oval J, Smedsrud M, Taetle R. Expression and regulation of the evi-1 gene in the human factor-dependent leukemia cell line, UCSD/AML1. *Leukemia* 1992; **6**: 446–451.
26 Oval J, Jones OW, Montoya M, Taetle R. Characterization of a factor-dependent acute leukemia cell line with translocation (3;3)(q21;q26). *Blood* 1990; **76**: 1369–1374.
27 Strefford JC, Foot NJ, Chaplin T, Neat MJ, Oliver RT, Young BD *et al.* The characterisation of the lymphoma cell line U937, using comparative genomic hybridisation and multiplex FISH. *Cytogenet Cell Genet* 2001; **94**: 9–14.
28 Gribble SM, Roberts I, Grace C, Andrews KM, Green AR, Nacheva EP. Cytogenetics of the chronic myeloid leukemia-derived cell line K562: karyotype clarification by multicolor fluorescence *in situ* hybridization, comparative genomic hybridization, and locus-specific fluorescence *in situ* hybridization. *Cancer Genet Cytogenet* 2000; **118**: 1–8.
29 Koeffler HP, Billing R, Lusis AJ, Sparkes R, Golde DW. An undifferentiated variant derived from the human acute myelogenous leukemia cell line (KG-1). *Blood* 1980; **56**: 265–273.
30 MacLeod RA, Dirks WG, Drexler HG. Early contamination of the Dami cell line by HEL. *Blood* 1997; **90**: 2850–2851.
31 Gallagher R, Collins S, Trujillo J, McCredie K, Ahearn M, Tsai S *et al.* Characterization of the continuous, differentiating myeloid cell line (HL-60) from a patient with acute promyelocytic leukemia. *Blood* 1979; **54**: 713–733.
32 Tsuchiya S, Yamabe M, Yamaguchi Y, Kobayashi Y, Konno T, Tada K. Establishment and characterization of a human acute monocytic leukemia cell line (THP-1). *Int J Cancer* 1980; **26**: 171–176.
33 Hamaguchi H, Suzukawa K, Nagata K, Yamamoto K, Yagasaki F, Morishita K. Establishment of a novel human myeloid leukaemia cell line (HNT-34) with t(3;3)(q21;q26), t(9;22)(q34;q11) and the expression of EVI1 gene, P210 and P190 BCR/ABL chimaeric transcripts from a patient with AML after MDS with 3q21q26 syndrome. *Br J Haematol* 1997; **98**: 399–407.
34 Matsuo Y, Adachi T, Tsubota T, Imanishi J, Minowada J. Establishment and characterization of a novel megakaryoblastic cell line, MOLM-1, from a patient with chronic myelogenous leukemia. *Hum Cell* 1991; **4**: 261–264.
35 Asou H, Suzukawa K, Kita K, Nakase K, Ueda H, Morishita K *et al.* Establishment of an undifferentiated leukemia cell line (Kasumi-3) with t(3;7)(q27;q22) and activation of the EVI1 gene. *Jpn J Cancer Res* 1996; **87**: 269–274.
36 Suzukawa K, Kodera T, Shimizu S, Nagasawa T, Asou H, Kamada N *et al.* Activation of EVI1 transcripts with chromosomal translocation joining the TCRVbeta locus and the EVI1 gene in human acute undifferentiated leukemia cell line (Kasumi-3) with a complex translocation of der(3)t(3;7;8). *Leukemia* 1999; **13**: 1359–1366.
37 Abo J, Inokuchi K, Dan K, Nomura T. p53 and N-ras mutations in two new leukemia cell lines established from a patient with multilineage CD7-positive acute leukemia. *Blood* 1993; **82**: 2829–2836.
38 Hamaguchi H, Nagata K, Yamamoto K, Fujikawa I, Kobayashi M, Eguchi M. Establishment of a novel human myeloid leukaemia cell line (FKH-1) with t(6;9)(p23;q34) and the expression of dek-can chimaeric transcript. *Br J Haematol* 1998; **102**: 1249–1256.
39 Hamaguchi H, Inokuchi K, Nara N, Nagata K, Yamamoto K, Yagasaki F *et al.* Alterations in the colorectal carcinoma gene and protein in a novel human myeloid leukemia cell line with trisomy 18 established from overt leukemia after myelodysplastic syndrome. *Int J Hematol* 1998; **67**: 153–164.
40 Pawson R, Dyer MJ, Barge R, Matutes E, Thornton PD, Emmett E *et al.* Treatment of T-cell prolymphocytic leukemia with human CD52 antibody. *J Clin Oncol* 1997; **15**: 2667–2672.
41 Piccaluga PP, Agostinelli C, Righi S, Zinzani PL, Pileri SA. Expression of CD52 in peripheral T-cell lymphoma. *Haematologica* 2007; **92**: 566–567.

42 Geissinger E, Bonzheim I, Roth S, Rosenwald A, Muller-Hermelink HK, Rudiger T. CD52 expression in peripheral T-cell lymphomas determined by combined immunophenotyping using tumor cell specific T-cell receptor antibodies. *Leuk Lymphoma* 2009; **50**: 1010–1016.
43 Lugthart S, Gröschel S, Beverloo HB, Kayser S, Valk PJ, van Zelderen-Bhola SL *et al.* Clinical, molecular, and prognostic significance of WHO type inv(3)(q21q26.2)/t(3;3)(q21;q26.2) and various other 3q abnormalities in acute myeloid leukemia. *J Clin Oncol* 2010; **28**: 3890–3898.
44 Stein S, Ott MG, Schultze-Strasser S, Jauch A, Burwinkel B, Kinner A *et al.* Genomic instability and myelodysplasia with monosomy 7 consequent to EVI1 activation after gene therapy for chronic granulomatous disease. *Nat Med* 2010; **16**: 198–204.
45 Yuasa H, Oike Y, Iwama A, Nishikata I, Sugiyama D, Perkins A *et al.* Oncogenic transcription factor Evi1 regulates hematopoietic stem cell proliferation through GATA-2 expression. *EMBO J* 2005; **24**: 1976–1987.
46 Treumann A, Lifely MR, Schneider P, Ferguson MA. Primary structure of CD52. *J Biol Chem* 1995; **270**: 6088–6099.
47 Ermini L, Secciani F, La Sala GB, Sabatini L, Fineschi D, Hale G *et al.* Different glycoforms of the human GPI-anchored antigen CD52 associate differently with lipid microdomains in leukocytes and sperm membranes. *Biochem Biophys Res Commun* 2005; **338**: 1275–1283.

Supplementary Information accompanies the paper on the Leukemia website (http://www.nature.com/leu)

Oncogene (2011) 30, 4194–4207

www.nature.com/onc

ORIGINAL ARTICLE

Sumoylation of MEL1S at lysine 568 and its interaction with CtBP facilitates its repressor activity and the blockade of G-CSF-induced myeloid differentiation

I Nishikata, S Nakahata, Y Saito, K Kaneda, E Ichihara, N Yamakawa and K Morishita

Division of Tumor and Cellular Biochemistry, Department of Medical Sciences, Faculty of Medicine, University of Miyazaki, Miyazaki, Japan

MEL1 **(MDS1/EVI1-like gene 1/*PRDM16*), which was identified as a gene near the chromosomal breakpoint in t(1;3)(p36;q21)-positive human acute myeloid leukemia cells, belongs to the PRDI-BF1-RIZ1 homologous (PR) domain (PRDM) family of transcription repressors. The short form of MEL1 (MEL1S), which lacks the PR-domain at the *N*-terminus, is the main form expressed in t(1;3)(p36;q21)-positive acute myeloid leukemia cells. The overexpression of MEL1S blocks granulocyte colony-stimulating factor (G-CSF)-induced myeloid differentiation in interleukin-3-dependent murine myeloid L-G3 cells. In this study, we show that treatment with the histone deacetylase inhibitor trichostatin A abolished the blockade of myeloid differentiation in L-G3 cells overexpressing MEL1S. The expression of MEL1S containing mutated CtBP-interacting motif (CIM) in L-G3 cells still blocked the myeloid differentiation induced by G-CSF. We found that the small ubiquitin-related modifier (SUMO) motif (SM) at lysine 568 (VKAE) adjacent to the CIM was necessary to obtain the maximum transcriptional repressor activity of MEL1S. L-G3 cells expressing MEL1S, and bearing mutated CIM and SM differentiated into granulocytes in response to G-CSF; this indicated that both the SUMO modification at lysine 568 and CtBP binding were required for MEL1S-mediated transcriptional repression and blockade of differentiation, which might be relevant for the process of leukemogenesis.**

Oncogene (2011) **30,** 4194–4207; doi:10.1038/onc.2011.132; published online 25 April 2011

Keywords: MEL1; sumoylation; CtBP; G-CSF

Introduction

Acute myeloid leukemia with reciprocal translocation t(1;3)(p36;q21) is frequently characterized by trilineage dysplasia, particularly dysmegakaryocytopoiesis, and a poor prognosis (Moir *et al.*, 1984; Bloomfield *et al.*, 1985; Welborn *et al.*, 1987). These clinical features are very similar to those of the 3q21q26 syndrome, which is characterized by a high expression of the ecotropic viral integration site-1 (*EVI1*) gene (Shimizu *et al.*, 2000). EVI1 (also called PR domain member 3 or PRDM3) is a zinc-finger transcription factor and belongs to the PRDI-BF1-RIZ1 homologous (PR) domain family (Morishita, 2007). We previously identified the MDS1/EVI1-like gene 1 (*MEL1*) as a member of the *EVI1* gene family and also as a PR domain family member (*PRDM16*); this gene is located near the chromosomal breakpoint at chromosome 1p36 of t(1;3)(p36;q21) (Mochizuki *et al.*, 2000; Shimizu *et al.*, 2000). PR-domain deficient forms of EVI1 and MEL1 (MEL1S) are upregulated in both types of leukemia (Mochizuki *et al.*, 2000; Nishikata *et al.*, 2003). We discovered that the overexpression of MEL1S in murine interleukin-3 (IL-3)-dependent myeloid L-G3 cells blocked the granulocytic differentiation induced by granulocyte colony-stimulating factor (G-CSF) (Nishikata *et al.*, 2003). Using the GAL4 DNA-binding domain (DBD) fused to MEL1 and MEL1S, we also identified that both MEL1 and MEL1S function as transcriptional repressors (Nishikata *et al.*, 2003).

EVI1 and MEL1 also belong to a family of transcription factors with *C*-terminal-binding protein (CtBP)-interacting motif (CIM) (Shimahara *et al.*, 2010). EVI1 has two CIMs, PFDLT (aa 553–559) and PLDLS (aa 584–590), and the repressor and cell-transforming functions of EVI1 are mediated by its CtBP-binding activity (Izutsu *et al.*, 2001). Moreover, MEL1/PRDM16 also has two CIMs, PFDLT (aa588–592) and PLDLS (aa 616–620), and was reported to directly interact with a CtBP co-repressor complex on the promoter of white fat-specific genes (Kajimura *et al.*, 2008).

CtBP was originally identified as a transcriptional co-repressor of the adenoviral E1A protein (Schaeper *et al.*, 1995). In addition, among transcription factors containing zinc-finger repeats, BKLF, ZEB1, ZEB2 (Shimahara *et al.*, 2010) and ZNF217 (Quinlan *et al.*, 2006) have been reported to have CIM. The CtBP co-repressor complex contains a number of epigenetic regulatory factors that mediate coordinated histone modification by deacetylation and methylation of histone H3

Correspondence: Dr K Morishita, Division of Tumor and Cellular Biochemistry, Department of Medical Sciences, Faculty of Medicine, University of Miyazaki, 5200 Kihara, Kiyotake, Miyazaki 889-1692, Japan.
E-mail: kmorishi@med.miyazaki-u.ac.jp
Received 25 November 2010; revised and accepted 19 March 2011; published online 25 April 2011

at lysine 9 and demethylation of histone H3 at lysine 4 (Chinnadurai, 2007). CtBP also recruits the small ubiquitin-related modifier (SUMO) and conjugates the E2 enzyme UBC9 and a SUMO E3 ligase (HPC2) (Kagey *et al.*, 2003). Therefore, it is possible that sumoylation might also be involved in CtBP-mediated transcriptional regulation.

In this study, we investigated whether the transcriptional repressor activity of MEL1 could mediate the blockade of the granulocytic differentiation of L-G3 cells induced by G-CSF. The L-G3 cells treated with the histone deacetylase (HDAC) inhibitor trichostatin A (TSA) overcame blockade of the G-CSF-induced differentiation by MEL1S expression. Here, the transcriptional repression by MEL1S is reported to be mediated by sumoylation and its interaction with CtBP. MEL1S interacted with the E2-conjugating enzyme UBC9, which led to sumoylation, and interacted with the transcriptional co-repressor CtBP. Site-directed mutagenesis and deletion analysis identified lysine 568 as a sumoylation site in MEL1S. Mutations of both the sumoylation site and the CIMs in MEL1S completely abrogated the repressor activity and released the MEL1S-induced differentiation block in L-G3 cells. Therefore, the transcriptional repressor activity of MEL1S is likely one of the important determinants in the development of leukemia.

Results

Combining G-CSF with TSA treatment overcomes the blockade of G-CSF-induced differentiation in murine L-G3 cells induced by MEL1S expression

We previously reported that the short form of MEL1 (MEL1S), a transcription factor that is specifically expressed in acute myeloid leukemia with the t(1;3) translocation, could block G-CSF-induced myeloid differentiation of L-G3, an IL-3-dependent myeloid leukemia cell line (Nishikata *et al.*, 2003). Because MEL1S works as a transcriptional repressor in hematopoietic cells, including L-G3 cells (Supplementary Figure 1), we initially investigated whether treatment of L-G3 cells with the HDAC inhibitor TSA prevents the blockade of G-CSF-induced differentiation by MEL1S expression. A series of L-G3 cell lines, consisting of parental cells or cells transfected with a Mock-vector (L-G3/Mock) or a MEL1S expression vector (L-G3/MEL1S), were cultured with IL-3, G-CSF or G-CSF with TSA for 6 days, and their cell growth, morphology and expression of myeloperoxidase (*Mpo*) and lactoferrin (*Lf*) (Friedman *et al.*, 1991), both of which are markers of granulocyte differentiation, were determined. At 6 days after treatment with G-CSF, most of the parental L-G3 cells and L-G3/Mock cells exhibited reduced cell growth, increased cell death, differentiation to granulocytes with multi-lobulated nuclei and expression of *Mpo* and *Lf*; however, the majority of L-G3/MEL1S cells grew well and remained undifferentiated myeloid cells with no *Mpo* and *Lf* expression (Figures 1a–d). At 6 days after treatment with G-CSF and TSA, the majority of the L-G3/MEL1S cells stopped growing and lost viability; the surviving cells differentiated into granulocytes and expressed *Mpo* and *Lf*. The L-G3/MEL1S cells treated with G-CSF and TSA survived 1–2 days longer than the G-CSF-treated control L-G3 cells, even though the surviving cells differentiated into mature granulocytes (Figures 1a and c). Therefore, TSA treatment, when combined with G-CSF, could release the blockade of granulocyte differentiation induced by MEL1S expression.

MEL1S lacking CtBP-interacting domain lost the transcriptional repressor activity

To determine the domain(s) of MEL1 that are responsible for transcriptional repression, we constructed a series of deletion mutants of MEL1S fused with the DBD of GAL4 (GAL4-DBD/MEL1) driven by the SV40 promoter. These mutants represent deletions of zinc-finger repeats 1–7 in the DBD1 (ΔDBD1), the proline-rich region (ΔPRR), the CtBP-interacting domain (CID) (ΔCID), the repressor domain (ΔRD), zinc-finger repeats 8–10 in the DBD2 (ΔDBD2) and the *C*-terminal acidic amino-acid cluster region (ΔCT) (Figure 2a). Either wild-type (WT) GAL4-DBD/MEL1S or a deletion mutant plasmid was transfected along with the pG5proLuc reporter plasmid into COS-7 cells, and the protein expression of each construct was confirmed by immunoblot analysis (Figure 2b). At 2 days after transfection, repression activity was measured by comparing the luciferase enzyme activities for each deletion construct to WT MEL1S as a reference. The repression was clearly reduced with MEL1S/ΔDBD1, MEL1S/ΔCID or MEL1S/ΔRD; MEL1S/ΔCID showed almost no repressor activity compared with WT MEL1S. Therefore, the CID may be the most important domain for the repressor activity of MEL1S.

Amino-acid substitutions in the MEL1S CIMs block G-CSF-induced myeloid differentiation

To evaluate whether the repressor activity of the CID of MEL1S is dependent on binding to the CtBP co-repressor, a MEL1S mutant carrying four amino-acid substitutions in the two CIMs (Shimahara *et al.*, 2010), which are located at amino-acids 588–592 (PFDLT) and 618–622 (PLDLS) (Figure 3a), was constructed. The aspartic acid and leucine at positions 560 and 561 in the first CIM (PFDLT) were replaced by alanine and serine (PFAST), and the aspartic acid and leucine at positions 660 and 661 in the second CIM (PLDLS) were replaced by alanine and serine (PLASS) to yield the CIM mutant (CIMmt) in the GAL4-DBD/MEL1 construct. To confirm the lack of CtBP-binding ability of the MEL1/CIMmt mutant, we transfected HA-tagged MEL1/WT, MEL1S/WT or MEL1S/CIMmt expression vectors with or without the FLAG-tagged CtBP2 expression vector into 293T cells. After immunoprecipitation using an anti-FLAG antibody, the precipitated proteins were detected using an anti-HA antibody, and CtBP2 was confirmed to bind MEL1 or MEL1S but not MEL1S/CIMmt (Figure 3b).

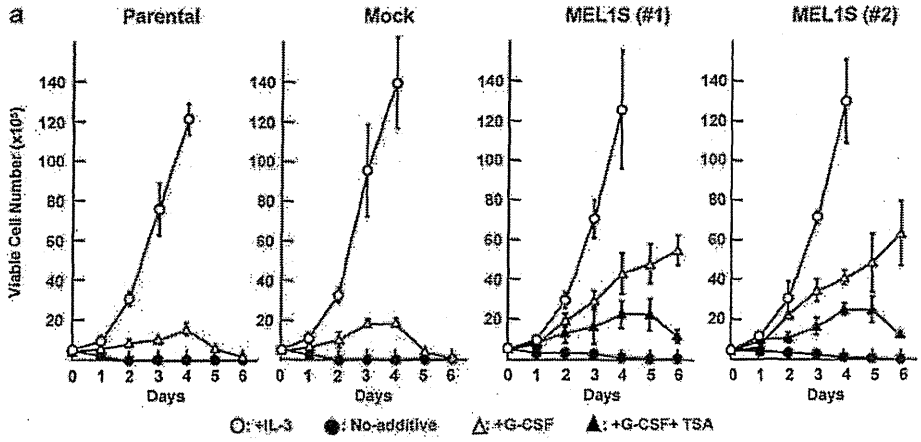
a
Parental
Mock
MEL1S (#1)
MEL1S (#2)
Viable Cell Number (x10⁴)
Days
O: +IL-3
●: No-additive
△: +G-CSF
▲: +G-CSF+ TSA

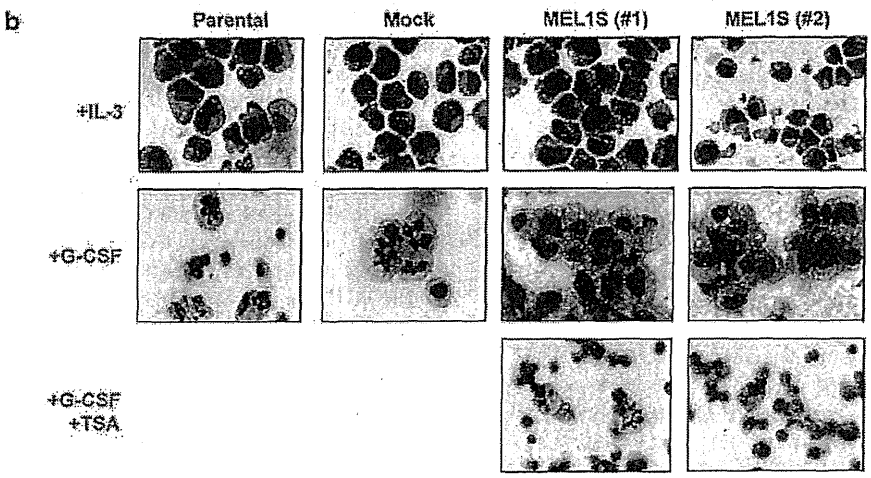
b
Parental
Mock
MEL1S (#1)
MEL1S (#2)
+IL-3
+G-CSF
+G-CSF
+TSA

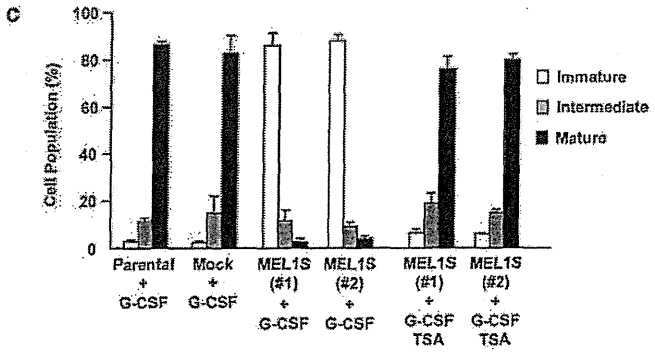
c
Cell Population (%)
Immature
Intermediate
Mature
Parental + G-CSF
Mock + G-CSF
MEL1S (#1) + G-CSF
MEL1S (#2) + G-CSF
MEL1S (#1) + G-CSF TSA
MEL1S (#2) + G-CSF TSA

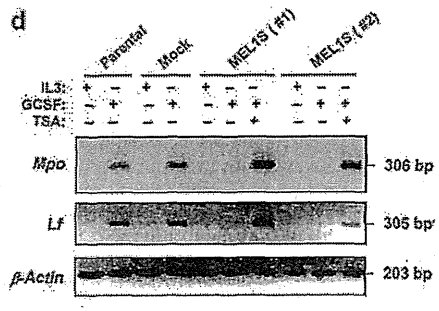
d
Parental
Mock
MEL1S (#1)
MEL1S (#2)
IL3:
GCSF:
TSA:
Mpo
Lf
β-Actin
306 bp
305 bp
203 bp

Next, a study was conducted on whether the expression of MEL1S/CIMmt could block G-CSF-induced myeloid differentiation of the L-G3 cell line. After transfection of the FLAG-tagged MEL1S/CIMmt expression vector into L-G3 cells, two L-G3/CIMmt cell lines were selected by G418 treatment and established. After confirming the MEL1 expression by immunoblot analysis with an anti-FLAG antibody (Figure 3c), the L-G3/MEL1S/CIMmt, L-G3 parental, L-G3/Mock and L-G3/MEL1S cells were treated with IL-3 or G-CSF for 6 days and their growth, cell morphology and expression of *Mpo* and *Lf* were determined. Parental L-G3 and L-G3/Mock control cells differentiated into granulocytes characterized by increased *MPO* and *Lf* mRNA levels on treatment with G-CSF, but the L-G3/MEL1S and MEL1S/CIMmt cell lines did not differentiate and remained immature myeloid cells (Figures 3d–f). Therefore, there is probably another important element for the inhibition of differentiation, apart from the CtBP-binding sites, within the CID.

Adjacent to the CtBP-interacting consensus sequence, MEL1S is sumoylated at K568 in an UBC9-dependent manner

Several transfection factors with CIM, such as ZEB1, ZEB2 and BKLF, were reported to be modified by sumoylation, facilitating the transcriptional repressor function by increasing the recruitment of HDAC. We searched for the SM ψKxE (where ψ is a large hydrophobic residue, K is the lysine to which the SUMO is conjugated, x is any amino acid and E is glutamic acid) (Rodriguez *et al*., 2001) in MEL1S using the SUMOplot analysis program (ABGENT, http://www.abgent.com/tools/sumoplot). There are seven high-probability putative SUMO consensus sites (scores over 0.69) in MEL1S (Supplementary Table 1). Of these, lysine 568 (AHNLL VKAE PKSPR) and lysine 85 (GLAEE LKPE GLGGG) have the highest probability of sumoylation (scores over 0.9), and lysine 568 is located just 20 amino-acid residues upstream of the CIM (PFDLT), within the CID.

To test whether MEL1S could be covalently modified by sumoylation, the FLAG-MEL1S expression vector was transfected with GFP-fused SUMO1 (GFP/SUMO1) and the Myc-tagged conjugating enzyme UBC-9 (Myc/UBC9) or with GFP/SUMO1 and a dominant negative form of Myc/UBC-9 with cysteine 93 mutated to serine (Giorgino *et al*., 2000) into 293T cells. The cell lysates were subjected to sodium dodecyl sulfate (SDS)–PAGE and blotted with an anti-FLAG antibody. As shown in Figure 4a, a slowly migrating band of MEL1S was detected only in the lysates from cells transfected with SUMO1 and UBC9, but not in those expressing SUMO1 and UBC9 (C93S). To confirm whether the slowly migrating band of MEL1S corresponded to a sumoylated form of MEL1S, 293T cells were transfected under the same conditions as above, and the cell lysates were immunoprecipitated with an anti-FLAG antibody to bring down MEL1S. The precipitated proteins were then detected using an anti-FLAG or anti-GFP antibody. As shown in Figure 4b, the slower migrating band of MEL1S was detected by both antibodies, suggesting that this form of the protein likely represents a sumoylated MEL1S.

Next, to determine the location of the sumoylation site in MEL1S, six FLAG-tagged deletion mutants of MEL1S (illustrated in Figure 2a) were transfected into 293T cells along with SUMO1 and UBC9; MEL1S protein levels were detected by immunoblotting with an anti-FLAG antibody. A sumoylated MEL1S band was detected in the lysates of cells transfected with all the MEL1S deletion mutants, except the MEL1S/ΔCID mutant (Figure 4c). Therefore, the lysine(s) modified by sumoylation might be located within the CID. Because lysine 568 (AHNLL VKAE PKSPR), which lies within the CID, is one of the candidate lysines with a high sumoylation probability score (Supplementary Table 1), a MEL1S mutant was constructed with arginine substituted for lysine at position 568 (K568R; sumoylation motif mutant or SMmt) to determine whether MEL1S was sumoylated at lysine 568 (Figure 4d). After co-transfection with FLAG-tagged MEL1S, MEL1S/ΔCID, MEL1S/SMmt or MEL1S/CIMmt and SUMO1 and UBC9, MEL1S was detected by blotting with an anti-FLAG antibody. Sumoylated MEL1S was detected in the lysates of cells transfected with MEL1/WT or MEL1S/CIMmt but not with MEL1S/ΔCID or MEL1S/SMmt (Figure 4e), suggesting that lysine 568 is the sumoylated lysine within the CID.

Figure 1 TSA promotes G-CSF-dependent granulocytic differentiation in L-G3 cells overexpressing MEL1S. (**a**) Growth curves of L-G3 cells infected with a *MEL1S* retrovirus. IL-3-dependent murine myeloid L-G3 cells stably expressed either FLAG-tagged MEL1S (L-G3/MEL1S, #1 and #2, which correspond to lanes 3 and 4 in Figure 3c) or the mock vector (L-G3/Mock). The parental cells were grown under different culture conditions. Viable cells were counted using the trypan-blue exclusion method at each time point. Each culture condition was marked at the bottom of the figure. Open or closed circles indicate the culture conditions using medium with or without IL-3, respectively, and open or closed triangles indicate medium with G-CSF or G-CSF + TSA, respectively. The error bars represent the s.d. of three independent experiments. (**b**) May-Grünwald-Giemsa staining of cytospin preparations of parental and infected L-G3 cells after cultivation in IL-3 (top panel), G-CSF (middle panel) or G-CSF + TSA (bottom panel) for 6 days. Pictures were taken at × 100 magnification. (**c**) Comparison of cell populations estimated by counting stained nuclei after 6 days of culture in different media. The graph shows the results from two independent experiments; in each experiment, more than 100 cells were surveyed under the microscope. After culture in medium containing G-CSF alone or G-CSF with TSA, the cells were classified into the following three categories: immature, intermediate and mature. The population of cells in each category is expressed as the percentage (%) of the total cells. (**d**) Detection of myeloperoxidase *(Mpo)* and lactoferrin *(Lf)* expression in L-G3 transformants and parental cells cultured in medium containing IL-3, G-CSF or G-CSF + TSA for 6 days. Semi-quantitative RT–PCR was performed using specific primers for *Mpo* or *Lf*. RT–PCR for *β-Actin* was performed to test for equal loading. The sizes of the PCR products for *Mpo, Lf* and *β-Actin* are 306, 305 and 203 bp, respectively.

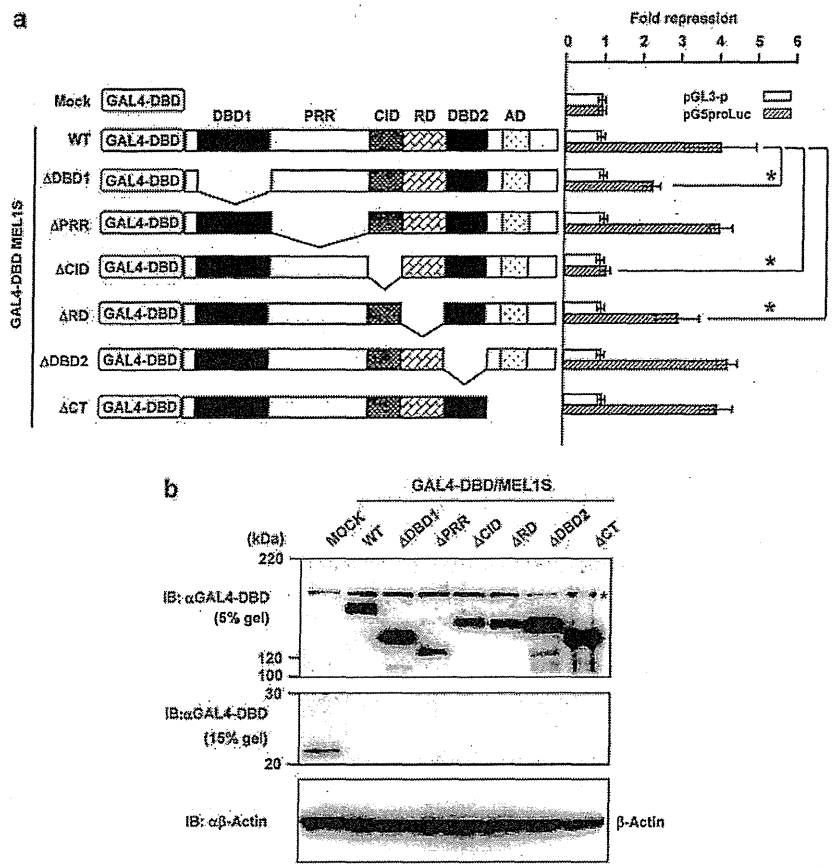

Figure 2 Transcriptional activities of MEL1S and the deletion mutants fused to the *C*-terminal end of the GAL4-DBD. (**a**) Repression activities of GAL4-DBD-fused MEL1S and its deletion mutants. COS-7 cells were co-transfected with the pGL3-promoter vector control (pGL3-p) or pG5proLuc with five consensus GAL4-binding sites (UAS) and the internal control plasmid pRL-MP together with the mock expression vector (GAL4-DBD), GAL4-DBD/MEL1S or the deletion mutants, as illustrated in Figure 2a. After 48 h of incubation, the cell extracts were prepared, and reporter activity was determined according to the manufacturer's instructions. Values of relative luciferase activity represent the mean ± s.d. of three independent transfections. $*P<0.05$ (Student's *t*-test). (**b**) The protein expression levels of transfected MEL1S and the deletion mutants in COS-7 cells were determined by immunoblotting using the anti-GAL4-DBD antibody. The expression of GAL4–DBD/MEL1S fusion proteins (top panel) and Mock constructs (middle panel) were analyzed by 5 and 15% SDS–PAGE, respectively. β-Actin was used as an internal control. Molecular weight markers are given in kilodaltons (kDa). Stars indicate nonspecific bands.

Figure 3 Forced expression of the MEL1S mutant harboring disrupted CIM blocks G-CSF-induced granulocytic differentiation. (**a**) Schematic illustration of human MEL1S and the mutant form of MEL1S. PRD indicates the PR domain; DBD1, DNA-binding domain 1; PRR, the proline-rich region; CID, the CtBP-interacting domain; RD, the repression domain; DBD2, DNA-binding domain 2; and AD, the acidic domain. MEL1S has two CIMs (PFDLT and PLDLS). The motifs reside in the CID of MEL1S. The two CIMs, PFDLT and PLDLS, were mutated to PFAST and PLASS, respectively, by site-directed mutagenesis. (**b**) MEL1S interacts with CtBP2 through the CIM. HA-tagged MEL1, MEL1S or MEL1S/CIM mutant was transiently expressed with FLAG-tagged CtBP2 in 293T cells. HA-tagged MEL1 proteins and FLAG-CtBP2 were immunoprecipitated using an anti-HA antibody and an anti-FLAG antibody, respectively. The precipitated proteins were separated by SDS–PAGE and MEL1, MEL1S, the CIM mutant and/or CtBP2 were detected by western blotting (top panels). The inputs of each assay are shown on the bottom panels. (**c**) Expression of MEL1S (FLAG/MEL1S/WT) and the mutant (FLAG/MEL1S/CIMmt and FLAG/MEL1S/SMmt/CIMmt) clones in retrovirally infected L-G3 cell lines. Cell extracts from L-G3 cells infected with retrovirus containing FLAG-tagged MEL1S or its mutants were subjected to immunoblotting using the anti-FLAG antibody. Expression of β-Actin, which served as an internal control, is shown in the lower panel. Molecular weight markers are given in kDa. (**d**) Growth curves of L-G3 cells infected with retrovirus encoding a *MEL1S* mutant harboring disrupted CIM. L-G3 cells stably expressing either FLAG-tagged MEL1S (L-G3/MEL1S), the CtBP interaction mutant (L-G3/MEL1S/CIMmt, #1 and #2, which correspond to lanes 5 and 6 in Figure 3c), or the mock vector (L-G3/Mock) and the parental cells were grown under different culture conditions. Viable cells were counted by the trypan-blue exclusion method at each time point. Each culture condition is marked at the bottom of the figure. Open or closed circles indicate the culture conditions using medium with or without IL-3, respectively, and open triangles indicate medium with G-CSF. The error bars represent the s.d. of three independent experiments. (**e**) May-Grünwald-Giemsa staining of cytospin preparations of parental and infected L-G3 cells after cultivation in medium containing IL-3 (top panel) or G-CSF (bottom panel) for 6 days. Pictures were taken at × 100 magnification. (**f**) Detection of *Mpo* and *Lf* expression in L-G3 transformants and parental cells cultured in medium containing IL-3 or G-CSF for 6 days. Semi-quantitative RT–PCR was performed using *Mpo*- or *Lf*-specific primers.

Both sumoylation and CtBP binding in the CID are required for the transcriptional repressor function of MEL1S

To examine whether the transcriptional repressor activity of MEL1S is dependent on both sumoylation and CtBP binding in the CID, SM and CIMs, SM and CIMs double mutants (SM/CIMmt) were constructed in a GAL4 DBD-fused MEL1S expression vector (Figure 5a). After confirmation of the protein expression of each MEL1S expression plasmid by western blotting

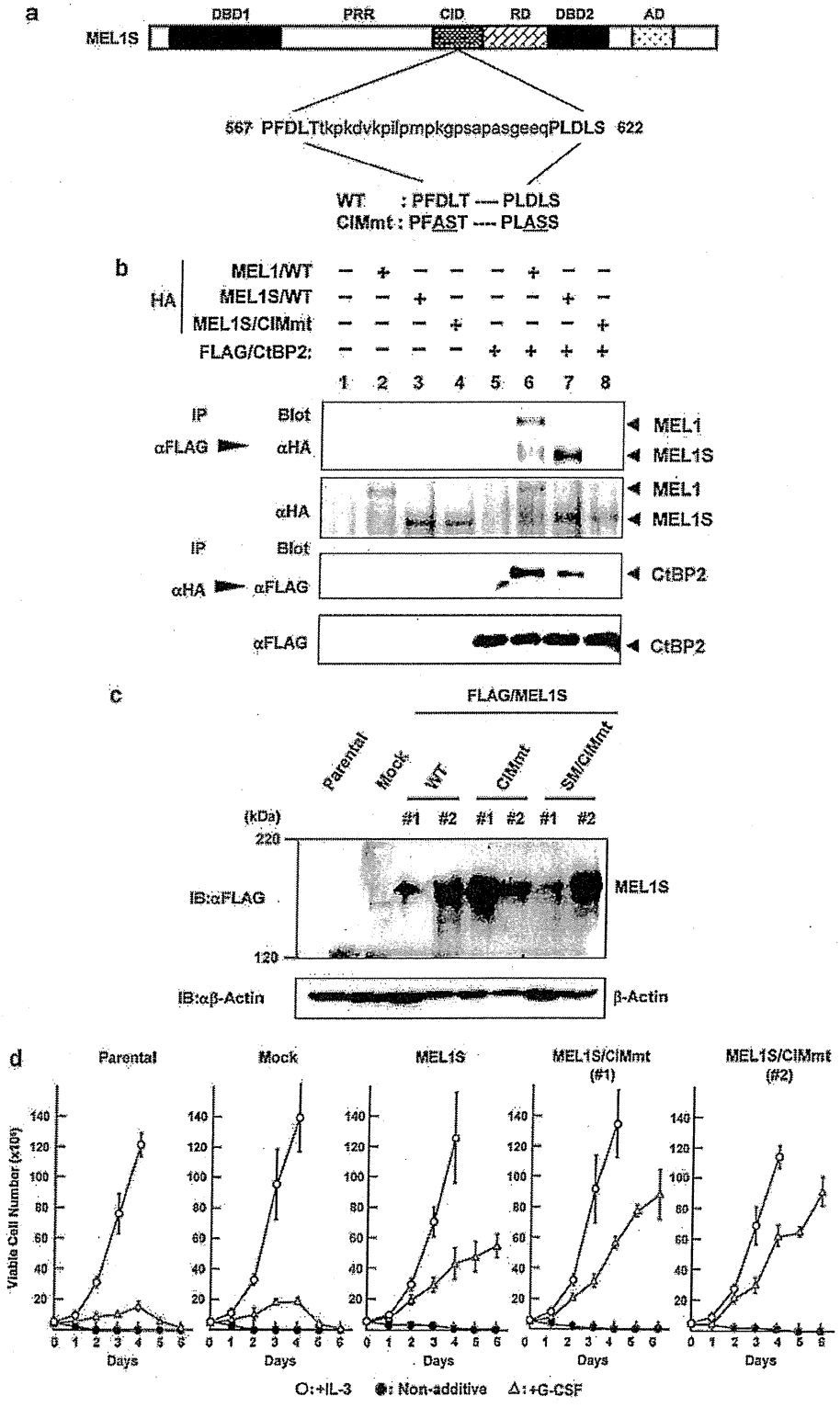

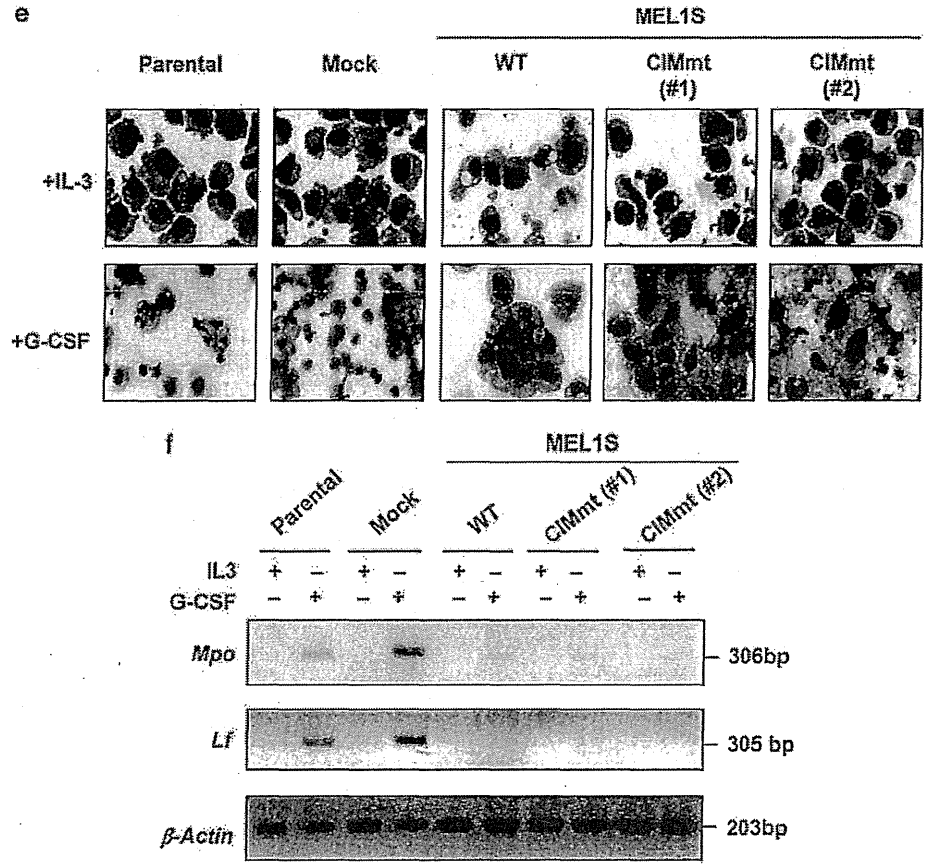

Figure 3 Continued.

(Figure 5b), each MEL1S construct (/WT,/ΔCID,/SMmt,/CIMmt, and SM/CIMmt) was analyzed for transcriptional repressor activity by co-transfection with the pG5proLuc reporter in COS-7 cells. MEL1S/WT-induced repression of the transcription by approximately fivefold, but MEL1S/ΔCID exhibited very little repressive activity (Figure 5a). The repressive activity of MEL1S/SMmt was slightly reduced compared with that of MEL1S/WT, and the activity of MEL1S/CIMmt was moderately reduced. Interestingly, the repression activity of MEL1S/SM/CIMmt was negligible, suggesting that both the sumoylation and the CtBP-binding property might contribute to the transcriptional repressor activity of MEL1S.

HDAC interacts with the sumoylated and CtBP-interacting regions in the CID of MEL1S

Because transcriptional repression by MEL1S may involve the recruitment of HDAC, the binding of HDAC to the SM and CIMs was assessed in the CID of MEL1S as EVI1 (Mitani, 2004; Maki *et al*., 2008). For this experiment, the expression vectors were constructed containing a GFP-fused CID (GFP/CID) containing various mutations, such as CID/SMmt, CID/CIMmt or CID/SM/CIMmt (Figure 6a), which contain the same amino-acid substitutions as in Figures 3a and 4d. These constructs were transfected with or without a FLAG-tagged HDAC2 expression vector into 293T cells, and the cell lysates were immunoprecipitated with an anti-FLAG M2 affinity gel. The precipitated proteins were detected using an anti-GFP antibody. The precipitated GFP/CID protein was clearly detected in the lysates of cells transfected with GFP/CID/WT, but the level of the GFP/CID protein was clearly decreased with the GFP/CID/SMmt and GFP/CID/CIMmt expression vectors (Figure 6b). Moreover, the GFP/CID/SM/CIMmt protein was not co-immunoprecipitated with FLAG-HDAC2, suggesting that HDAC failed to interact with GFP/CID/SM/CIMmt. Therefore, HDAC could bind to both the SM and the CIM in the CID.

Expression of MEL1S with double mutants of SM and CIM in L-G3 cells did not block granulocyte differentiation induced by G-CSF

Finally, to determine whether the combined repressor activity by sumoylation and CtBP-binding ability might be related to the differentiation blockade by MEL1S, a MEL1S expression vector containing SMmt and CIMmt (SM/CIMmt) was constructed and transfected into L-G3 cells. After the establishment of the MEL1S/SM/

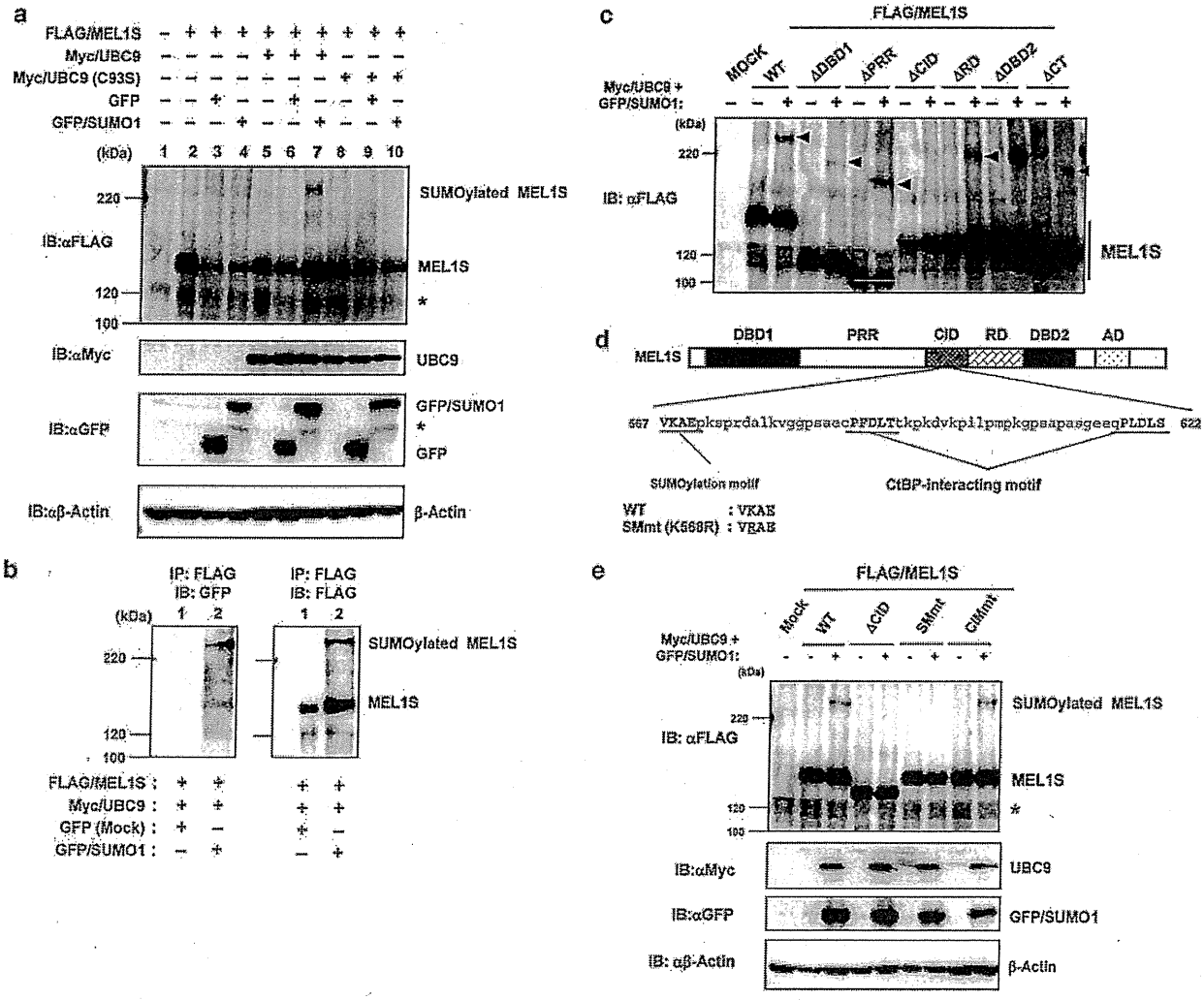

Figure 4 MEL1S was sumoylated at lysine 568 in a SM adjacent to the CIM. (**a**) Sumoylation of MEL1S is dependent on UBC9. Cells (293T) were co-transfected with expression plasmids encoding FLAG/MEL1S, Myc-tagged UBC9 or Myc-tagged dominant negative UBC9 (the C93S mutant) and/or GFP/SUMO1. The cell lysates were analyzed by western blotting using an anti-FLAG antibody. Expression of UBC9, SUMO1 and β-Actin is shown in the three lower panels. Molecular weight markers are given in kDa. (**b**) Identification of sumoylated MEL1S by immunoblot analysis. Flag-tagged MEL1S with Myc/UBC9 was transfected along with control GFP or GFP-fused SUMO1 into 293T cells. After immunoprecipitation with an anti-FLAG antibody, sumoylated MEL1S was detected using an anti-GFP antibody for GFP/SUMO1 in the left panel. In the right panel, after immunoprecipitation out of the same samples with the anti-FLAG antibody, MEL1S was identified using an anti-FLAG antibody. (**c**) The detection of the more slowly migrating band of MEL1S as a sumoylated form of MEL1S by transfection of expression vectors containing each MEL1S mutant is indicated in Figure 2a, with or without Myc/UBC9 and GFP/SUMO1 expression plasmids. Cells (293T) were transfected under the same conditions as in Figure 4a, and the cell lysates were analyzed by western blotting using an anti-FLAG antibody. Molecular weight markers are given in kDa. Stars indicate sumoylated MEL1S. (**d**) Schematic illustration of human MEL1S and the mutant form of MEL1S. MEL1S has a SM (VKAE) adjacent to two CIMs (PFDLT and PLDLS). These motifs are located in the CID of MEL1S. The SM was mutated to VRAE by site-directed mutagenesis. Abbreviations are the same as in Figure 3a. (**e**) The MEL1S K568R mutant cannot be sumoylated. An expression plasmid encoding either FLAG/MEL1S (WT), the CID-deleted MEL1S mutant (ΔCID), the SM-abolished mutant (SMmt) or the CIM-abolished mutant (CIMmt) was transfected with or without Myc/UBC9 and GFP/SUMO1 expression plasmids into 293T cells, and the cell lysates were analyzed by western blotting using an anti-FLAG antibody. Expression of UBC9, SUMO1 and β-Actin is shown in the three lower panels.

CIMmt #1 and #2 cell lines (Figure 3c), a series of L-G3 cell lines expressing WT or mutant MEL1S were cultured with a vehicle, IL-3 or G-CSF for 6 days. The major difference between the control and MEL1S/SM/CIMmt cell lines was the different patterns of cell growth in cultures supplemented with G-CSF. In response to G-CSF, parental and L-G3/Mock control cells grew slowly and differentiated into granulocytes, but L-G3 cells with MEL1S or MEL1S/CIMmt expression grew without differentiating into granulocytes (Figures 7a and b). The patterns of cell growth in the two MEL1S/SM/CIMmt cell lines were very similar to those of the parental and L-G3/Mock cell lines, and both MEL1S/SM/CIMmt cell lines showed granulocyte

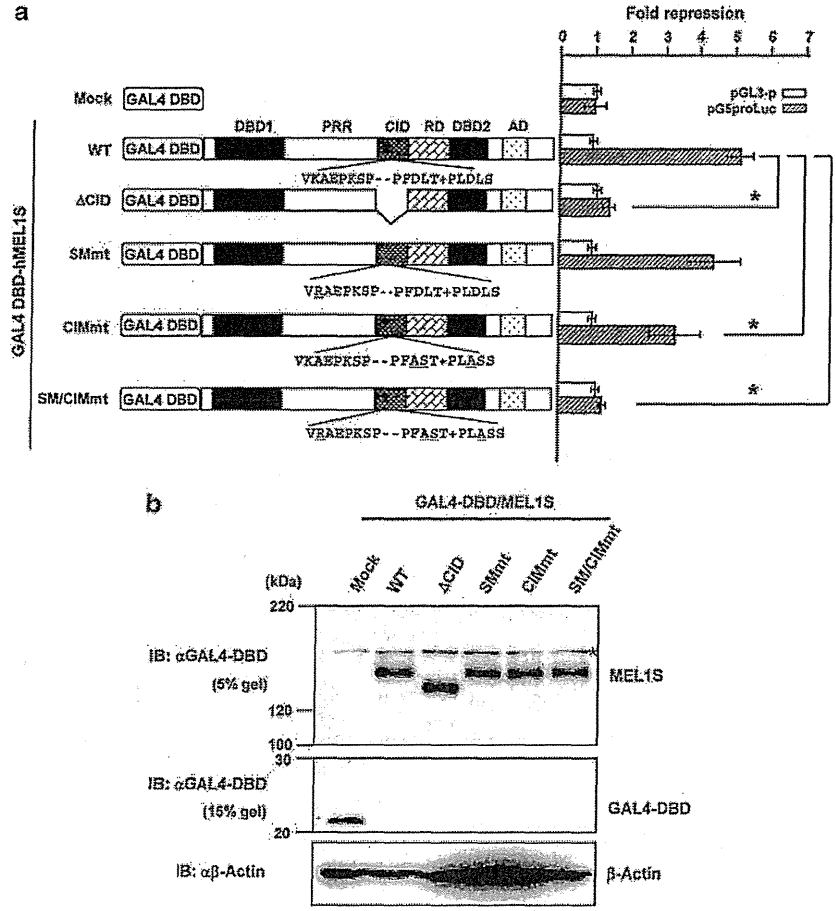

Figure 5 Mutation of both the SM and the CIMs in MEL1S abolishes its transcriptional repressor activity. (**a**) Transcriptional repressor activities of GAL4–DBD-fused MEL1S and mutant forms of MEL1S. COS-7 cells were co-transfected with the luciferase reporter vector (pGL3-p or pG5proLuc) and an internal control plasmid, pRL-MP, along with an expression vector for GAL4–DBD/MEL1S or its mutants, as illustrated in Figure 5a. The reporter assay was carried out 48 h after transfection. Values of relative luciferase activity represent the mean ± s.d. of three independent transfections. $*P<0.05$ (Student's *t*-test). (**b**) The protein expression levels of transfected MEL1S and the deletion mutants in COS-7 cells were determined by western blotting using the anti-GAL4-DBD antibody. The star indicates a nonspecific band.

differentiation with multi-lobulated nuclei after 6 days of culture with G-CSF. To confirm granulocyte differentiation, the expression of *MPO* and *Lf* in these cells was analyzed 6 days after treatment with G-CSF by reverse-transcription–PCR (Figure 7d). The expression of *MPO* and *Lf* was detected in parental, Mock and MEL1S/SM/CIMmt #1 and #2 cells. The lower level of *MPO* expression in the MEL1S/SM/CIMmt cells may reflect the presence of a small number of immature myeloid cells (Figures 7c). To confirm the results, these experiments were repeated in the IL-3-dependent murine myeloid cell line 32Dcl3 expressing either WT MEL1S or MEL1S/SM/CIMmt. The forced expression of WT MEL1S was found, but MEL1S/SM/CIMmt did not result in the inhibition of G-CSF-induced differentiation in 32Dcl3 cells (Supplementary Figures 2a, b, c, d and e). To confirm whether MEL1S was sumoylated in L-G3 cells, stable -L-G3 cell lines expressing WT or mutant MEL1S were transfected with Myc/UBC9 and GFP/SUMO1 expression plasmids, and sumoylation levels were determined by western blot analysis with the anti-FLAG antibody. A slowly migrating band corresponded to sumoylated MEL1S and was detected in the lysates from MEL1S/WT and MEL1S/CIM cells but not from MEL1S/SM/CIMmt #1 or #2 cells (Figure 7e). These data suggest that the ability of MEL1S to block differentiation was primarily dependent on the transcriptional repression activity mediated by both sumoylation and CtBP binding in the CID of MEL1S.

Discussion

In this study, we showed that sumoylation of and CtBP interaction with the CID cooperatively mediated transcriptional repression activity of the MEL1 zinc-finger protein; in addition, MEL1 transcriptional repression activity was found to be essential for its blockade of G-CSF-induced granulocyte differentiation of

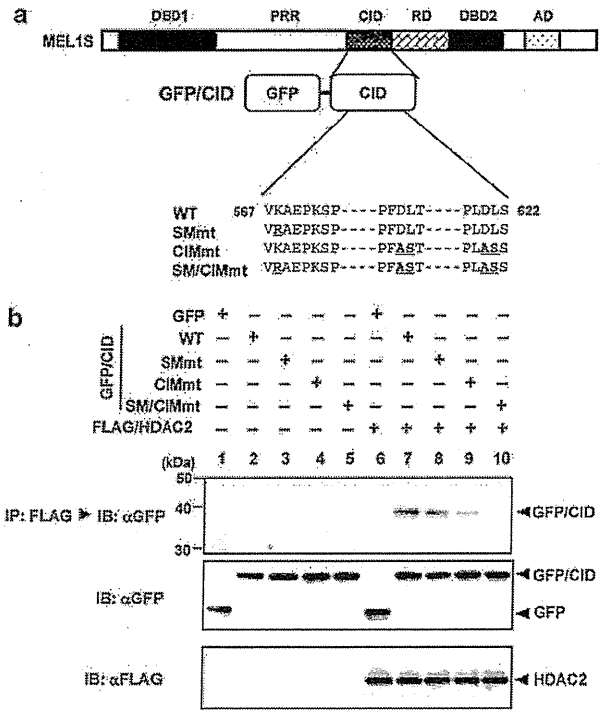

Figure 6 Mutation of both the SM and the CIMs abolishes the recruitment of HDAC2 to the CID of MEL1S. (**a**) Schematic illustration of human MEL1S and GFP-fused CID. Amino-acid substitutions in the SM and/or the CIM are shown at the bottom. Abbreviations are the same as those in Figure 3a. (**b**) Neither the SM nor the CIM-disrupted CID can interact with HDAC2. Either a GFP/CID fusion (WT, SMmt, CIMmt, SM/CIMmt) vector or the mock (GFP) vector was co-transfected with or without a vector expressing FLAG/HDAC2 into 293T cells. The cell lysates were subjected to immunoprecipitation with the anti-FLAG antibody and blotted with an anti-GFP antibody. WT GFP/CID and the three mutant forms that interacted with HDAC2 are shown in the top panel. The direct western blotting of CID using the anti-GFP antibody and of HDAC2 using the anti-FLAG antibody are shown in the middle and bottom panels, respectively.

murine IL-3-dependent L-G3 cells. We have identified an important SUMO acceptor site at lysine 568, which lies just adjacent to the CIM, within the CID. Amino-acid substitutions in the SM and CIM of MEL1S completely abrogated the protein's transcriptional repression activity and its recruitment of the HDAC complex. Finally, L-G3 cells were stably transfected with a double mutant of MEL1S (SM/CIMmt) and differentiated into granulocytes on treatment with G-CSF. Although the sumoylation status of MEL1S has not been shown in acute myeloid leukemia cells, these data demonstrate that the overexpression of MEL1 in a myeloid cell line could inhibit G-CSF-induced granulocyte differentiation through transcriptional repression of yet unidentified genes, and this pathway may contribute to myeloid leukemogenesis.

Several C_2H_2 zinc-finger transcription factors contain CIM and SM that have an important role in modulating transcriptional repressor activity. BKLF, a Krüppel-like C_2H_2 zinc-finger transcription factor expressed in erythroid cells, contains a CIM and two SMs (Perdomo *et al.*, 2005). The SUMO site at K10 resides in the repression domain and is located 41 amino-acids upstream from the CIM, and the other SUMO site (K198) is located between the repressor domain and the zinc-finger DBD (Perdomo *et al.*, 2005). Sumoylation and interaction with CtBP synergistically enhanced the transcriptional repression activity of BKLF (Perdomo *et al.*, 2005). Both ZEB1 and ZEB2 have been reported to be sumoylated on two conserved lysine residues; one SUMO site (K774 in ZEB1 and K866 in ZEB2) is located adjacent to a CIM, and another site (K347 in ZEB1 and K391 in ZEB2) is located between the first zinc-finger cluster (composed of zinc-finger repeats 1–4) and the Smad-binding domain. Mutations of these two sumoylated lysine residues in ZEB1 caused a loss of the transcriptional repression function of ZEB1, and the DNA binding ability of ZEB1 was shown to be dependent on the sumoylation of the two lysine residues in a chromatin immunoprecipitation assay (Kuppuswamy *et al.*, 2008). Conversely, the sumoylation of ZEB2 attenuates its transcriptional repression of E-cadherin, which is caused by reduced binding to the co-repressor CtBP (Long *et al.*, 2005). Although the function of sumoylation of zinc-finger transcription factors with CIM differs from one transcription factor to the next, sumoylation of the BKLF and MEL1S transcription factors may facilitate recruitment of the HDAC complex to increase transcriptional repression activity; however, a study of BKLF did not show an increased recruitment of the HDAC complex upon sumoylation (Perdomo *et al.*, 2005).

Hematopoietic cell differentiation is regulated by lineage-specific transcription factors that function in a mutually antagonistic manner. For example, MafB and c-Myb function as antagonists for each other in a balance between macrophage differentiation and myeloid progenitor expansion. C-Myb suppresses MafB-driven differentiation through sumoylation of MafB (Tillmanns *et al.*, 2007); conversely, c-Myb is also affected by sumoylation. TRAF7, a SUMO ligase, sequesters c-Myb in the cytoplasm by increasing its sumoylation (Morita *et al.*, 2005). Thus, sumoylation is one of the important regulatory events in cellular differentiation and proliferation. Interestingly, MEL1/PRDM16 is one of transcription factors in the regulation of brown fat versus white fat/skeletal muscle differentiation (Seale *et al.*, 2008). In myoblasts and preadipocytes, MEL1/PRDM16 promotes the expression of brown fat cell-selective genes by co-activating the transcriptional activity of PGC-1α/1β and PPARα/γ through direct interaction (Kajimura *et al.*, 2008). In addition, MEL1/PRDM16 represses the expression of white fat- or skeletal muscle-specific genes by association with the co-repressor CtBP (Kajimura *et al.*, 2009). Although the mechanisms underlying the molecular switch that changes MEL1/PRDM16 from a transcriptional activator to a repressor have not yet been elucidated, sumoylation may have an important role in this transcriptional switch. Given that the overexpression of MEL1S was found to block the granulocytic

differentiation of L-G3 myeloid leukemia cells, inhibition of MEL1S sumoylation through targeting of tissue-specific SUMO ligases may present a novel strategy in myeloid leukemia. The SUMO ligases for MEL1S in hematopoietic stem cells and/or myeloid progenitor cells remain to be identified.

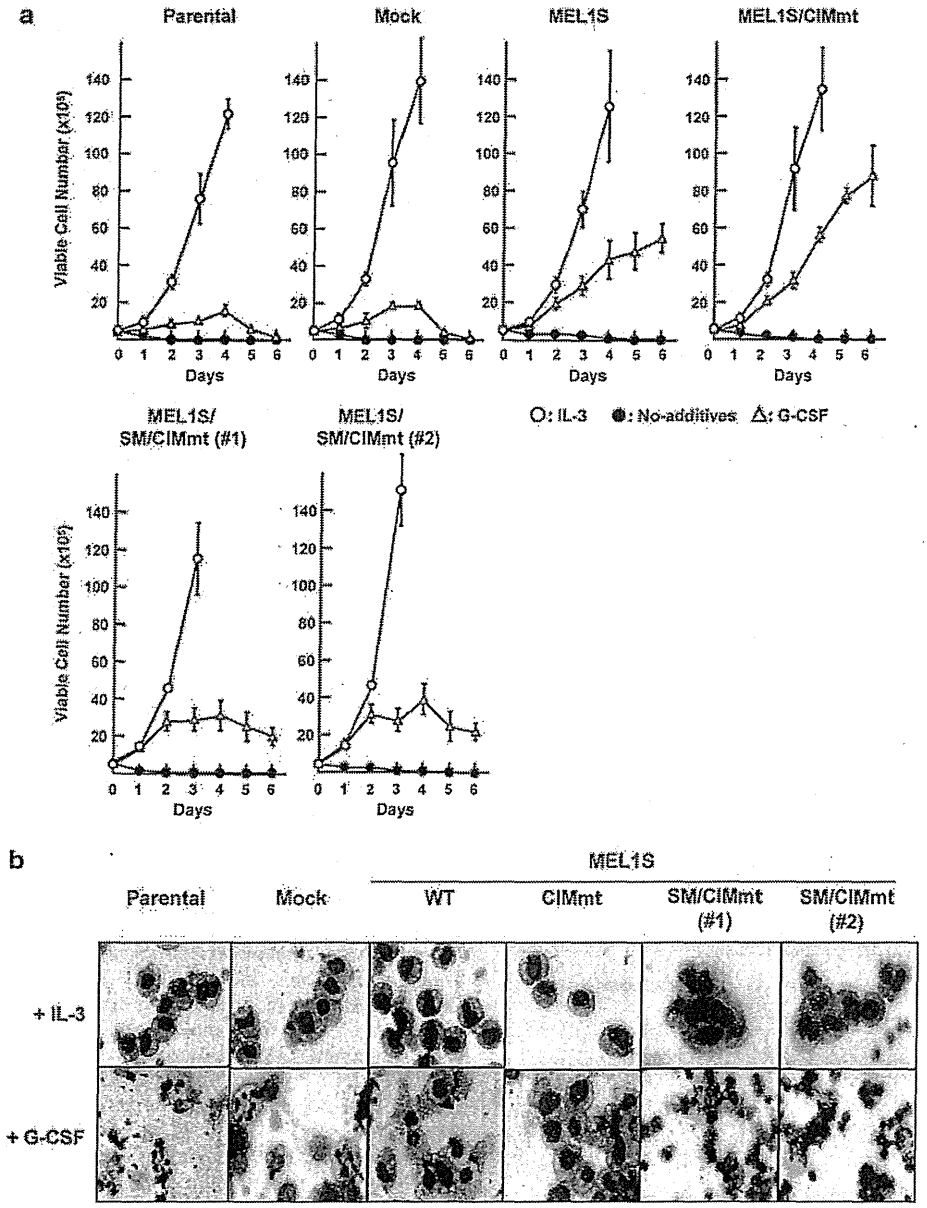

Figure 7 L-G3 transformants overexpressing SM and/or CIM motif-disrupted MEL1S mutants differentiate into granulocytes in response to G-CSF. (**a**) Growth curves of L-G3 cells infected with retrovirus with *MEL1S* mutants lacking a SM or two CIMs. L-G3 cells stably expressing either FLAG-tagged MEL1S (L-G3/MEL1S), the CtBP interaction mutant (L-G3/MEL1S/CIMmt), the mutant with both the SM and the CIMs disrupted (L-G3/MEL1S/SM/CIMmt, #1 and #2, corresponding to lanes 7 and 8 in Figure 3c) or the mock vector (L-G3/Mock) and the parental cells were grown under different culture conditions. Viable cells were counted using the trypan-blue exclusion method at each time point. Open or closed circles indicate the culture conditions using medium with or without IL-3, respectively, and open triangles indicate medium with G-CSF. The error bars represent the s.d. of three independent experiments. (**b**) May-Grünwald-Giemsa staining was performed on parental and infected L-G3 cells after cultivation in medium containing IL-3 (top panel) or G-CSF (bottom panel) for 6 days. Pictures were taken at × 100 magnification. (**c**) Comparison of cell populations among various transformants of L-G3 cells estimated by counting stained nuclei after 6 days of culture in medium with G-CSF. The data show the results from two independent experiments and are presented as in Figure 1c. (**d**) Semi-quantitative RT–PCR assessment of *Mpo* and *Lf* mRNA levels was performed on RNA isolated from cells cultured in medium with IL-3 or G-CSF for 6 days. (**e**) The MEL1S in the L-G3 transformants was sumoylated. The transient transfection of Myc/UBC9 and GFP/SUMO1 expression plasmids into L-G3 transformants was performed by Amaxa Nucleofection systems (Wako), and the cell lysates were analyzed by western blotting using an anti-FLAG antibody. The expression of UBC9, SUMO1 and β-Actin is shown in the three lower panels.

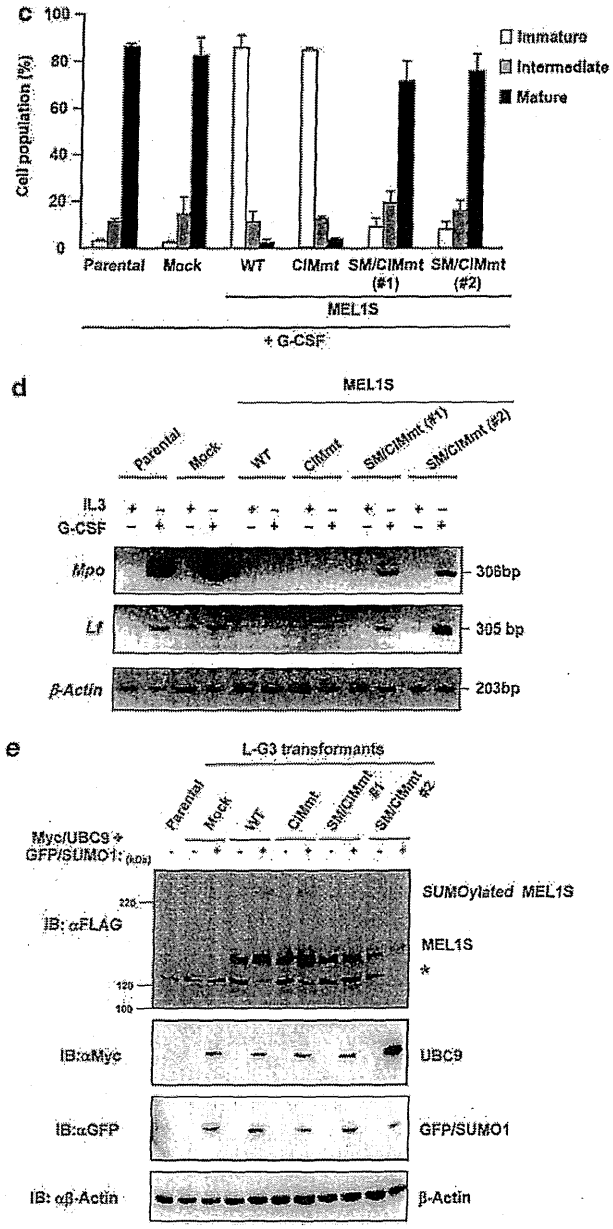

Figure 7 Continued.

Materials and methods

Plasmid constructions

To construct human *MEL1S* expression vectors, a FLAG- or a hemagglutinin (HA)-epitope tagged, short-form MEL1 lacking an *N*-terminal PR domain (*MEL1S*) (Mochizuki *et al.*, 2000; Nishikata *et al.*, 2003) was placed under the control of a cytomegalovirus (CMV) promoter in a mammalian expression vector pCMV26 (Sigma-Aldrich, St Louis, MO, USA) (pFLAG-MEL1S or pHA-MEL1S). To construct the human *MEL1* expression vector, a HA-epitope tagged, long-form MEL1 with a PR domain (Mochizuki *et al.*, 2000; Nishikata *et al.*, 2003) was inserted into the pCMV26 (pHA-MEL1). Using the In-Fusion cloning kit (Clontech, Mountain View, CA, USA), deletion mutants of MEL1S, including MEL1S/ΔDBD1 (DBD1, containing the 1–7 zinc-finger repeats, aa 40–264), MEL1S/ΔPRR (proline-rich region, aa 265–522), MEL1S/ΔCID (CID, aa 523–644), MEL1S/ΔRD (repression domain, aa 645–766), MEL1S/ΔDBD2 (DBD2, containing the 8–10 zinc-finger repeats, aa 767–887) and MEL1S/ΔCT (*C*-terminal region containing acidic domain, aa 893–1072), were generated by PCR amplification of human *MEL1S* complementary DNA lacking each domain structure (Figure 2a). To generate MEL1S mutants with amino-acid substitutions, a mutant with lysine 568 replaced by arginine in the SM (MEL1S/SMmt with K568R), the CIM mutant MEL1S-CIMmt (PFAST at aa 588-592 and PLASS at aa 618-622), and the double mutant (MEL1S/SM/CIMmt) were generated using a Quick Change II site-directed mutagenesis kit (Stratagene, La Jolla, CA, USA). The GAL4 DBD-fused MEL1S expression constructs with various deletions and amino acid replacements were cloned into the pM expression vector (Clontech). The murine CtBP2 expression vector, pFLAG-CtBP2, contained a full-length murine *CtBP2* (kindly provided by Dr Crossley; Turner and Crossley, 1998) cloned into the FLAG-epitope tag expression vector pFLAG-Mock. The human UBC9 expression vectors, pMyc-UBC9 and pMyc-UBC9DN, contain full-length human *UBC9* and the dominant negative mutant (C93S), respectively, cloned into the Myc-epitope tag expression vector pMyc-Mock. The human SUMO expression vector pGFP-SUMO1 contains full-length human *SUMO-1* and was cloned into the pGFP-epitope tag expression vector pGFP-Mock. A series of CID fragments from MEL1S containing WT CID (CID/WT) or CID with a series of amino-acid substitutions (CID/SMmt, CID/CIMmt and CID/SM/CIMmt) were cloned into the pGFP-epitope tag expression vector pGFP-Mock. The chicken HDAC2 expression vector pFLAG-HDAC2 and the Mock vector were kindly provided by Dr Y Takami (University of Miyazaki, Miyazaki, Japan). For the reporter gene assay, the pG5proLuc vector was used as a reporter expressing firefly luciferase (Nishikata *et al.*, 2003). The TK promoter in the pG4.74 *Renilla* luciferase internal control vector (Promega, Madison, WI, USA) was replaced with the minimum promoter (MP) from the pGL4.23 firefly luciferase reporter vector (Promega) to generate pRL-MP.

Mammalian cell culture, transfection and infection

Human embryonic kidney 293T (DuBridge *et al.*, 1987), BOSC23 (Pear *et al.*, 1993) and simian kidney COS-7 cells (Gluzman, 1981) were maintained in Dulbecco's modified Eagle's medium (DMEM, Wako, Osaka, Japan) supplemented with 10% fetal bovine serum (FBS, Biofluids, Camarillo, CA, USA). IL-3-dependent murine myeloid cell lines, L-G3 (Kinashi *et al.*, 1991) and 32Dcl3 (Greenberger *et al.*, 1983; Migliaccio *et al.*, 1989) were maintained in RPMI 1640 (Wako) with 10% FBS and 5 ng/ml murine IL-3 (mIL-3, Kirin Brewery Co., Tokyo, Japan). The cells were grown in 5% CO_2 at 37 °C. Transfections were carried out using the Hilymax transfection reagent (DOJINDO, Kumamoto, Japan), according to the manufacturer's instructions. Transfection studies of L-G3 transformants for sumoylation assays and of 32Dcl3 cells for the generation of stable transformants were carried out using the Amaxa Nucleofection systems (Wako), according to the manufacturer's instructions. Cells were harvested 48 h after transfection for further analysis.

Retroviral infections

To generate L-G3 clones stably expressing WT human MEL1S and two of its mutants (MEL1S/CIMmt and MEL1S/SM/CIMmt), the respective complementary DNA sequences

were subcloned into the retroviral vector pLXSN (Clontech). Infectious retroviral particles bearing FLAG-tagged MEL1S/WT, MEL1S/CIMmt, or MEL1S/SM/CIMmt were prepared by transfection of the virus-producing BOSC23 cells with each retroviral expression vector. Neomycin-resistant clones were screened for expression of the FLAG-tagged proteins by immunoblot analysis using an anti-FLAG rabbit polyclonal antibody (Sigma-Aldrich).

Proliferation and differentiation assays

The L-G3 or 32Dcl3 stable cell lines were seeded at 1×10^5 cells/well in a 6-well dish and incubated for 24 h. The cells were subsequently washed twice in RPMI 1640 and incubated with 5 ng/ml mIL-3, 5 ng/ml G-CSF, 5 ng/ml G-CSF and 3 ng/ml TSA (Wako) or no growth factor for 6 (L-G3) or 9 days (32Dcl3). The morphological observations were studied by cytospinning the cells onto glass slides and staining with May-Grünwald-Giemsa solution (Merck, Darmstadt, Germany). For the measurement of viable cell numbers, live cells were counted at indicated intervals using trypan blue exclusion (Sigma-Aldrich). Murine IL-3 and G-CSF were kindly provided by Kirin Brewery Co. All results were reproduced twice.

Immunoprecipitation and immunoblot analyses

Transfected cells were directly lysed in SDS sample buffer, boiled, resolved on 5 or 10% SDS–polyacrylamide gels, and transferred to polyvinylidene fluoride (PVDF) membranes (Immobilon-P, Millipore, Billerica, MA, USA). For immunoprecipitation assays, 5×10^6 cells were washed in phosphate-buffered saline and solubilized with 450 µl of radioimmune precipitation assay (RIPA) buffer (50 mM Tris-HCl, pH 7.5, 150 mM NaCl, 5 mM EDTA, and 1% Triton X-100), which was supplemented with a protease inhibitor cocktail (Sigma-Aldrich). After centrifugation, the supernatants were incubated with 50 µl of anti-Flag M2 affinity gel (Sigma-Aldrich) overnight with rotation at 4 °C. The resins were washed three times with RIPA buffer, and proteins were eluted in SDS sample buffer. The detection of FLAG-, HA-, Myc- and GFP-tagged proteins was carried out using rabbit anti-Flag (1:1000, Sigma-Aldrich), rat monoclonal anti-HA (1:1000, 3F10, Roche, Manheim, Germany), mouse monoclonal anti-Myc (1:1000, 9B11, Cell Signaling Technology, Danvers, MA, USA) and rabbit anti-GFP (1:1000, MBL, Nagoya, Japan) antibodies. Mouse monoclonal anti-GAL4 DNA-BD (1:2000, Clontech), rabbit anti-MEL1 DBD1 (1–7 zinc-finger cluster) and DBD2 (8–10 zinc-finger cluster, 1:1000) antibodies (Nishikata *et al.*, 2003) were also used, and a mouse monoclonal anti-β-Actin antibody (1:5000, AC15, Sigma-Aldrich) was used to provide an internal loading control. Horseradish peroxidase-linked swine anti-rabbit, rabbit anti-rat (DakoCytomation Denmark A/S, Glostrup, Denmark), and sheep anti-mouse (GE Healthcare, Little Chalfont, England) immunoglobulins were used as secondary antibodies. Immunoreactive proteins were visualized on LAS-3000 (Fuji-film, Tokyo, Japan) using a Lumi-Light Plus western blotting substrate (Roche). All results were reproduced twice.

Reverse-transcriptase–PCR

Total RNA was extracted from each cell using Trizol reagents (Invitrogen, Carlsbad, CA, USA) and converted to complementary DNA using AMV reverse transcriptase (Takara, Shiga, Japan). The complementary DNA was used as a template for PCR performed by ExTaq polymerase (Takara), and the primers used were as follows: for mouse *Mpo*, forward 5′-CGCTTCTCCTTCTTCACTGG-3′ and reverse 5′-CTGCC ATTGTCTTGGAATCG-3′; for mouse *Lf*, forward 5′-AAAC AAGCATCGGGATTCCAG-3′ and reverse 5′-ACAATGC AGTCTTCCGTGGTG-3′; and for mouse *β-Actin*, forward 5′-TTCCTTCTTGGGTATGGAAT-3′ and reverse 5′-GAGC AATGATCTTGATCTTC-3′.

Reporter gene assay

Reporter gene assays were carried out using a GAL4-responsive artificial promoter-luciferase plasmid (pG5proLuc) (Nishikata *et al.*, 2003). Briefly, COS-7 cells were transfected in 12-well plates with 2 µg of DNA, which included the indicated reporter constructs and expression vectors, as well as 100 ng of pRL-MP plasmid as an indicator of transfection efficiency. The luciferase activities (firefly luciferase for the reporter and *Renilla* luciferase for the indicator) were measured using the Dual-Luciferase Assay System (Promega). All transfections were carried out in triplicate. The data obtained were compared with the control and statistically analyzed by Student's *t*-test.

Conflict of interest

The authors declare no conflict of interest.

Acknowledgements

This work was supported in part by Grants-in-Aid for Scientific Research of Priority Area from the Ministry of Education, Culture, Sports, Science and Technology in Japan.

References

Bloomfield CD, Garson OM, Volin L, Knuutila S, de la Chapelle A. (1985). t(1;3)(p36;q21) in acute nonlymphocytic leukemia: a new cytogenic-clinicopathologic association. *Blood* **66**: 1409–1413.

Chinnadurai G. (2007). Transcriptional regulation by C-terminal binding proteins. *Int J Biochem Cell Biol* **39**: 1593–1607.

DuBridge RB, Tang P, Hsia HC, Phai-Mooi L, Miller JH, Calos MP. (1987). Analysis of mutation in human cells by using Epstein-Barr virus shuttle system. *Mol Cell Biol* **7**: 379–387.

Friedman AD, Krieder BL, Venturelli D, Rovera G. (1991). Transcriptional regulation of two myeloid-specific genes, myeloperoxidase and lactoferrin, during differentiation of the murine cell line 32Dcl3. *Blood* **78**: 2426–2432.

Giorgino F, de Robertis O, Laviola L, Montrone C, Perrini S, McCowen K *et al.* (2000). The sentrin-conjugating enzyme mUBC9 interacts with transient transfection GLUT4 and GLUT1 glucose transporters and regulates transporter levels in skeletal muscle cells. *Proc Natl Acad Sci USA* **97**: 1125–1130.

Gluzman Y. (1981). SV40-transformed simian cells support the replication of early SV40 mutants. *Cell* **23**: 175–182.

Greenberger JS, Sakakeeny MA, Humphries RK, Eaves CJ, Eckner RJ. (1983). Demonstration of permanent factor-dependent multipotential (erythroid/neutrophil/basophil) hematopoietic progenitor cell line. *Proc Natl Acad Sci USA* **80**: 2931–2935.

Izutsu K, Kurokawa M, Imai Y, Maki K, Mitani K, Hirai H. (2001). The corepressor CtBP interacts with Evi-1 to repress transforming growth factor beta signaling. *Blood* **97**: 2815–2822.

Kagey MH, Melhuish TA, Wotton D. (2003). The polycomb protein Pc2 is a SUMO E3. *Cell* **113**: 127–137.

Kajimura S, Seale P, Kubota K, Lunsford E, Frangioni JV, Gygi SP *et al.* (2009). Initiation of myoblast to brown fat switch by a PRDM16-C/EBP-b transcriptional complex. *Nature* **460**: 1154–1159.

Kajimura S, Seale P, Tomaru T, Erdjument-Bromage H, Cooper MP, Ruas JL *et al.* (2008). Regulation of the brown and white fat gene programs through a PRDM16/CtBP transcriptional complex. *Genes Dev* **22**: 1397–1409.

Kinashi T, Lee HL, Ogawa M, Tohyama K, Tashiro K, Fukunaga R *et al.* (1991). Premature expression of the macrophage colony-stimulating factor receptor on a multipotential stem cell line does not alter differentiation lineages controlled by stromal cells used for coculture. *J Exp Med* **173**: 1267–1279.

Kuppuswamy M, Vijayalingam S, Zhao LJ, Zhou Y, Subramanian T, Ryerse J *et al.* (2008). Role of the PLDLS-binding cleft region of CtBP1 in recruitment of core and auxiliary components of the corepressor complex. *Mol Cell Biol* **28**: 269–281.

Long J, Zuo D, Park M. (2005). Pc2-mediated SUMOylation of Smad-interacting protein 1 attenuates transcriptional repression of E-cadherin. *J Biol Chem* **280**: 35477–35489.

Maki K, Yamagata T, Mitani K. (2008). Role of the *RUNX1-EVI1* fusion gene in leukemogenesis. *Cancer Sci* **99**: 1878–1883.

Migliaccio G, Migliaccio AR, Kreider BL, Rovera G, Adamson JW. (1989). Transcriptional regulation of two myeloid-specific genes, myeloperoxidase and lactoferrin, during differentiation of the murine cell line 32D C13. *J Cell Biol* **109**: 833–841.

Mitani K. (2004). Molecular mechanisms of leukemogenesis by AML1/EVI-1. *Oncogene* **23**: 4263–4269.

Mochizuki N, Shimizu S, Nagasawa T, Tanaka H, Taniwaki M, Yokota J *et al.* (2000). A novel gene, *MEL1*, mapped to 1p36.3 is highly homologous to the *MDS1/EVI1* gene and is transcriptionally activated in t(1;3)(p36;q21)-positive leukemia cells. *Blood* **96**: 3209–3214.

Moir DJ, Jones PAE, Pearson J, Ducan JR, Cook P, Buckle VJ. (1984). A new translocation, t(1;3)(p36;q21), in myelodysplastic disorders. *Blood* **64**: 553–555.

Morishita K. (2007). Leukemogenesis of the EVI1/MEL1 gene family. *Int J Hematol* **85**: 279–286.

Morita Y, Kanei-Ishii C, Nomura T, Ishii S. (2005). TRAF7 sequesters c-Myb to the cytoplasm by stimulating its SUMOylation. *Mol Biol Cell* **16**: 5433–5444.

Nishikata I, Sasaki H, Iga M, Tateno Y, Imayoshi S, Asou N *et al.* (2003). A novel EVI1 gene family, *MEL1*, lacking a PR domain (MEL1S) is expressed mainly in t(1;3)(p36;q21)-positive AML and blocks G-CSF-induced myeloid differentiation. *Blood* **102**: 3323–3332.

Pear WS, Nolan GP, Scott ML, Baltimore D. (1993). Production of high-titer helper-free retroviruses by transient transfection. *Proc Natl Acad Sci USA* **90**: 8392–8396.

Perdomo J, Verger A, Turner J, Crossley M. (2005). Role for SUMO modification in facilitating transcriptional repression by BKLF. *Mol Cell Biol* **25**: 1549–1559.

Quinlan KGR, Nardini M, Verger A, Francescato P, Yaswen P, Corda D *et al.* (2006). Specific recognition of ZNF217 and other zinc finger proteins at a surface groove of C-terminal binding proteins. *Mol Cell Biol* **26**: 8159–8172.

Rodriguez MS, Dargemont C, Hay RT. (2001). SUMO-1 conjugation *in vivo* requires both a consensus modification motif and nuclear targeting. *J Biol Chem* **276**: 12654–12659.

Schaeper U, Boyd JM, Verma S, Uhlmann E, Subramanian T, Chinnadurai G. (1995). Molecular cloning and characterization of a cellular phosphorprotein that interacts with a conserved C-terminal domain of adenovirus E1A involved in negative modulation of oncogenic transformation. *Proc Natl Acad Sci USA* **92**: 10467–10471.

Seale P, Bjok B, Yang W, Kajimura S, Chin S, Kuang S *et al.* (2008). PRDM16 controls a brown fat/skeletal muscle switch. *Nature* **454**: 961–967.

Shimahara A, Yamakawa N, Nishikata I, Morishita K. (2010). Acetylation of lysine 564 Adjacent to the C-terminal binding protein-binding motif in EVI1 is crucial for transcriptional activation of *GATA2*. *J Biol Chem* **285**: 16967–16977.

Shimizu S, Suzukawa K, Kodera T, Nagasawa T, Abe T, Taniwaki M *et al.* (2000). Identification of breakpoint cluster regions at 1p36.3 and 3q21 in hematologic malignancies with t(1;3)(p36;q21). *Genes Chromosomes Cancer* **27**: 229–238.

Tillmanns S, Otto C, Jaffray E, Roure CD, Bakri Y, Vanhille L *et al.* (2007). SUMO modification regulates MafB-driven macrophage differentiation by enabling Myb-dependent transcriptional repression. *Mol Cell Biol* **27**: 5554–5564.

Turner J, Crossley M. (1998). Cloning and characterization of mCtBP2, a co-repressor that associates with basic Krüppel-like factor and other mammalian transcriptional regulators. *EMBO J* **17**: 5129–5140.

Welborn JL, Lewis JP, Jenks H, Walling P. (1987). Diagnostic and prognostic signification of t(1;3)(p36;q21) in the disorders of hematopoiesis. *Cancer Genet Cytogenet* **28**: 277–285.

Supplementary Information accompanies the paper on the Oncogene website (http://www.nature.com/onc)

Biochemical and Biophysical Research Communications 416 (2011) 239–245

Contents lists available at SciVerse ScienceDirect

Biochemical and Biophysical Research Communications

journal homepage: www.elsevier.com/locate/ybbrc

Angiopoietin1 contributes to the maintenance of cell quiescence in EVI1^{high} leukemia cells

Emi Ichihara, Kazuko Kaneda, Yusuke Saito, Norio Yamakawa, Kazuhiro Morishita *

Division of Tumor and Cellular Biochemistry, Department of Medical Sciences, Faculty of Medicine, University of Miyazaki, Miyazaki, Japan

ARTICLE INFO

Article history:
Received 8 October 2011
Available online 18 October 2011

Keywords:
EVI1
AML
Ang1
p18
Cell cycle

ABSTRACT

Ecotropic viral integration site-1 (EVI1) is an oncogenic transcription factor in human acute myeloid leukemia (AML) associated with poor prognosis. Because the drug-resistance of leukemia cells is partly dependent on cell quiescence in the bone marrow niche, EVI1 may be involved in cell cycle regulation in leukemia cells. As a candidate regulator of the cell cycle in leukemia cells with high EVI1 expression (EVI1^{high}), we analyzed angiopoietin1 (Ang1), which is a down-regulated gene in EVI1-deficient mice and is involved in the quiescence of hematopoietic stem cells. The results of real-time PCR analyses showed that Ang1 is highly expressed in leukemia cell lines and primary AML cells with EVI1^{high} expression. Introduction of shRNA against EVI1 into EVI1^{high} leukemia cells down-regulated Ang1 expression. Moreover, knockdown of Ang1 in EVI1^{high} leukemia cells promoted cell cycle progression and down-regulated the CDK inhibitor p18 (INK4c). Treatment with a decoy Tie2/Fc protein also down-regulated the expression of p18. These results suggest that Ang1/Tie2 signaling may suppress cell cycle progression via maintenance of G0/G1 phase through up-regulation of p18 expression. This mechanism may help to maintain EVI1^{high} leukemia cells in the bone marrow niche and promote resistance to anti-cancer drugs.

1. Introduction

The murine ecotropic viral integration site-1 (EVI1) gene was isolated from a common site of retroviral insertion in AKXD murine myelogenous leukemias [1,2]. The homologous human gene EVI1 is located on chromosome 3q26, and chromosomal abnormalities at 3q26 lead to aberrant expression of EVI1 in myeloid malignancies, including acute myeloid leukemia (AML), myelodysplastic syndrome (MDS), and blastic crisis of chronic myeloid leukemia (CML) [3,4]. AML with high expression of EVI1 (EVI1^{high}) accounts for approximately 8–10% of all cases of AML, and it exhibits a poor prognosis because of resistance to chemotherapy [5–7]. The gene expression profiles of EVI1^{high} AML patients are quite similar to those of control CD34^{+} cells [6], and furthermore, analysis of EVI1-deficient mice has shown that EVI1 is required for the maintenance of hematopoietic stem cells (HSCs), suggesting that EVI1^{high} leukemia cells may have stem cell-like phenotypes.

We and other groups have shown that EVI1 is predominantly expressed both in embryonic HSCs and HSCs in adult bone marrow [8–10]. EVI1 maintains the self-renewal capacity of embryonic HSCs by activating Gata2 transcription [11], and ablation of EVI1 in adult bone marrow also leads to a significant decrease in HSCs [12]. Taken together, these results suggest that EVI1 is indispensable for HSC maintenance and that EVI1 may also play an important role in the maintenance of cell quiescence as stem cell-like phenotypes in leukemia cells, thereby contributing to their chemoresistance.

In this manuscript, we focused on angiopoietin1 (Ang1) as a candidate gene whose high expression may be involved in the maintenance of cell quiescence in EVI1^{high} leukemia cells. Ang1 was identified as a ligand of the tyrosine kinase receptor Tie2 [13,14], and it belongs to the angiopoietin family, which also includes Ang2, Ang3, and Ang4. Ang1 and Ang4 activate the Tie2 receptor as agonists, whereas Ang2 and Ang3 act as antagonists [15,16]. Interactions between Ang1 and the receptor tyrosine kinase Tie2 promote HSC quiescence and are important for the maintenance of long-term repopulation in vivo [17,18]. In our previous study, Ang1 expression was found to be down-regulated in embryonic HSCs from EVI1-deficient mice, as was Gata2 [11]. Therefore, we hypothesized that the expression of Ang1 in EVI1^{high} leukemia cells might be regulated by EVI1 and that Ang1 would promote cell quiescence in EVI1^{high} leukemia cells.

In this study, we initially examined the expression of Ang1 in leukemia cells and found that Ang1 was strongly expressed in leukemia cell lines and primary AML cells with EVI1^{high} expression.

* Corresponding author. Address: Division of Tumor and Cellular Biochemistry, Department of Medical Sciences, Faculty of Medicine, University of Miyazaki, 5200 Kihara, Kiyotake, Miyazaki, Japan. Fax: +81 985 85 2401.
E-mail address: kmorishi@medmiyazaki-u.ac.jp (K. Morishita).

0006-291X/$ - see front matter © 2011 Published by Elsevier Inc.
doi:10.1016/j.bbrc.2011.10.061

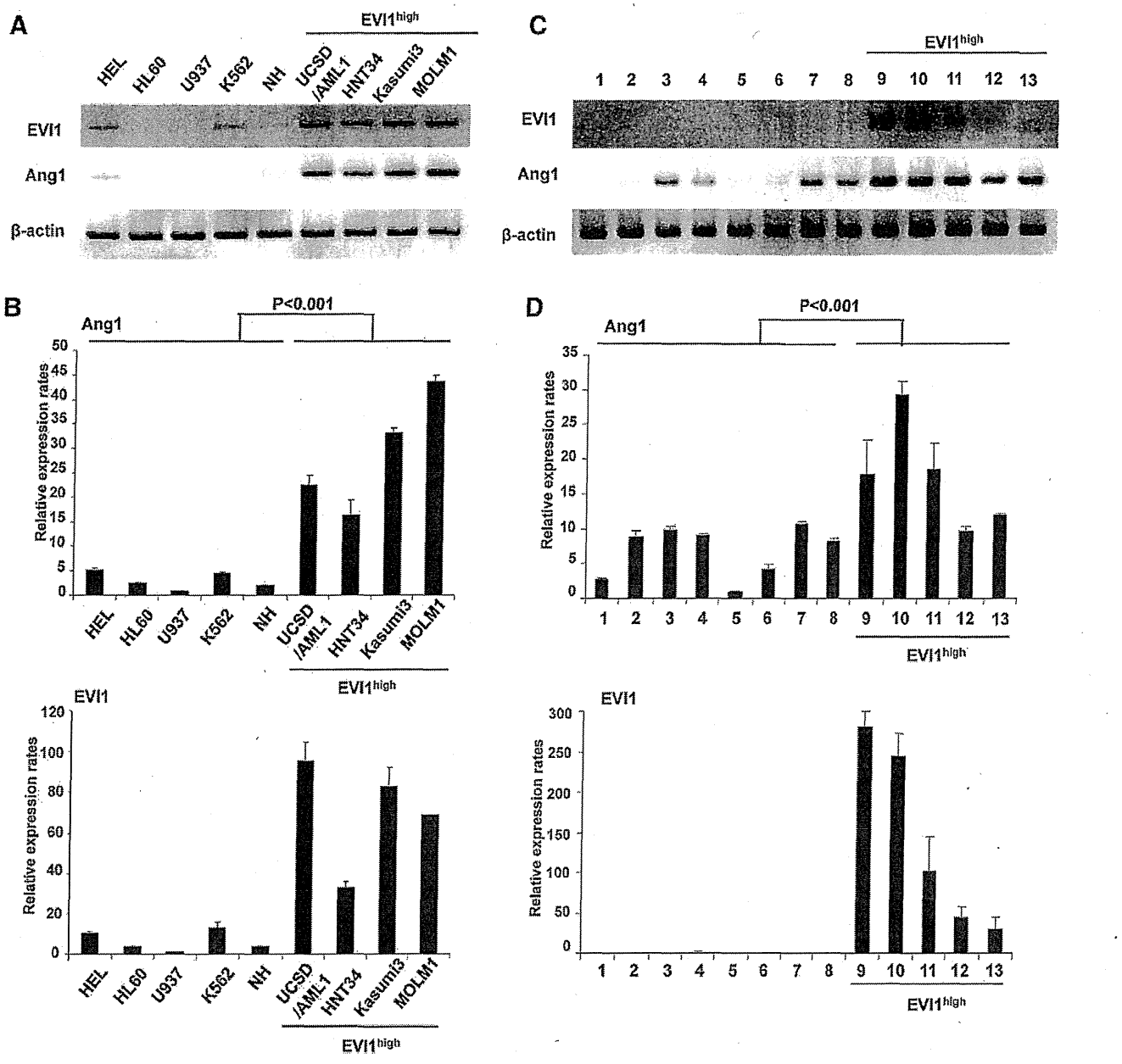

Fig. 1. Ang1 is highly expressed in EVI1^{high} leukemia cells. (A) Semi-quantitative reverse-transcription PCR (RT-PCR) analysis of EVI1 and Ang1 in various types of human leukemia cell lines. (B) Quantitative real-time RT-PCR analysis of EVI1 and Ang1 in leukemia cell lines. The data are presented as relative fold changes compared with the expression level in U937 cells. The data are expressed as the mean ± standard deviation (s.d.). Student's *t*-test was used for statistical analysis. (C) Semi-quantitative RT-PCR analysis of EVI1 and Ang1 in AML patient samples. (D) Quantitative real-time RT-PCR analysis of EVI1 and Ang1 in AML patient samples. The data are presented as relative fold changes compared with the expression in sample No. 5. The data are expressed as the mean ± s.d. Student's *t*-test was used for statistical analysis.

Introduction of shRNA targeting EVI1 into EVI1^{high} leukemia cells resulted in down-regulation of Ang1 expression. Ang1-knockdown experiments revealed that Ang1 suppresses cell cycle progression via maintenance of G0/G1 phase in EVI1^{high} leukemia cells. Moreover, knockdown of Ang1 expression and treatment with a Tie2 inhibitor (chimeric Tie2/Fc protein) down-regulated CDK inhibitor p18 (INK4c) expression. Therefore, Ang1/Tie2 signaling may contribute to cell quiescence through up-regulation of p18 expression in EVI1^{high} leukemia cells. This may enhance the maintenance of EVI1^{high} leukemia cells with resistance to chemotherapy in the bone marrow niche.

2. Materials and methods

2.1. Cell lines

UCSD/AML1 [19,20], HNT34 [21], and Kasumi-3 [22] cells were cultured in RPMI 1640 (Wako, Osaka, Japan) supplemented with 10% fetal calf serum (FCS) and 1 ng/mL human granulocyte–macrophage colony stimulating factor (hGM-CSF). HEL [23], HL60 [24], U937 [25], K562 [26], NH and MOLM1 [27] cells were cultured in RPMI 1640 supplemented with 10% FCS. 293T cells were cultured in DMEM (Wako) supplemented with 10% FCS. Detailed information

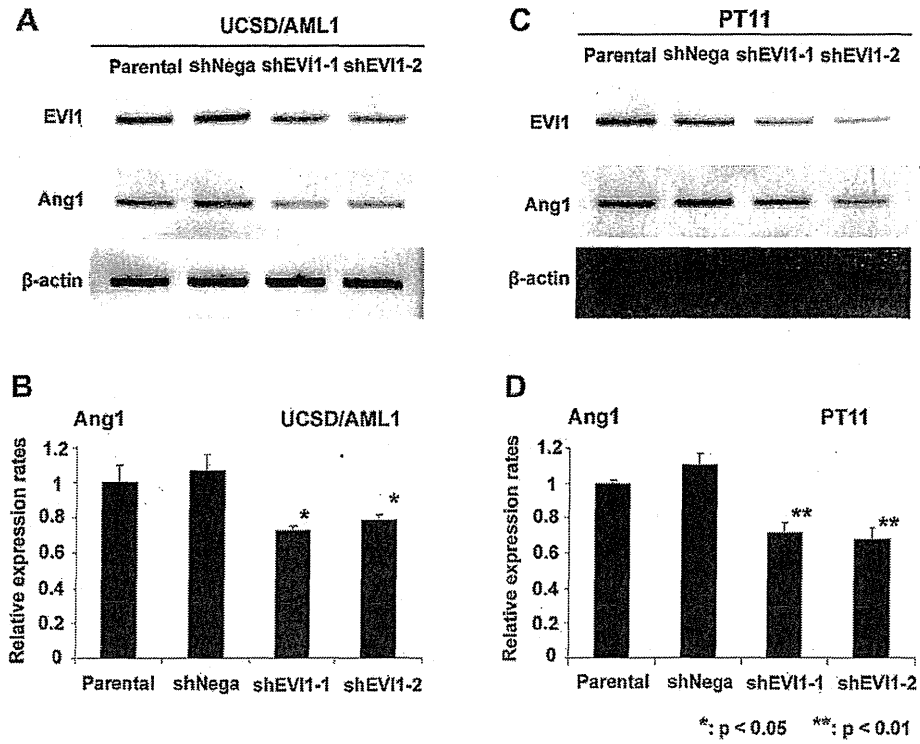

Fig. 2. Knockdown of EVI1 leads to down-regulation of Ang1 gene expression. (A) Small hairpin RNA (shRNA) against EVI1 was introduced into UCSD/AML1 cells to generate AML1/shEVI1-1, AML1/shEVI1-2, and AML1/shNega cell lines. shNega was used as a non-silencing control. Semi-quantitative RT-PCR analysis of EVI1 and Ang1 in parental UCSD/AML1 cells, AML1/shNega cells, and AML1/shEVI1-1 and -2 cells. (B) Quantitative real-time RT-PCR analysis of EVI1 and Ang1 in parental UCSD/AML1 cells, AML1/shNega cells, and AML1/shEVI1-1 and -2 cells. The data are presented as relative fold changes compared with the expression in parental UCSD/AML1 cells. The data are expressed as the mean ± s.d. Student's *t*-test was used for statistical analysis (*$p < 0.05$). (C) shRNA against EVI1 (shEVI1-1 or -2) was introduced into primary AML cells from a patient (PT11). Semi-quantitative RT-PCR analysis of EVI1 and Ang1 in parental PT11 cells, PT11/shNega cells, and PT11/shEVI1-1 and -2 cells. (D) Quantitative real-time RT-PCR analysis of EVI1 and Ang1 in parental PT11 cells, PT11/shNega cells, and PT11/shEVI1-1 and -2 cells. The data are presented as relative fold changes compared with the expression in parental PT11 cells. The data are expressed as the mean ± s.d. Student's *t*-test was used for statistical analysis (**$p < 0.01$).

about the cell lines was presented previously [28]. Briefly, UCSD/AML1, HNT34, Kasumi-3, and MOLM1 cells each have chromosome 3q26 abnormalities with high expression of EVI1, whereas HEL, HL60, U937, K562, and NH cells do not have 3q26 abnormalities and show low expression of EVI1.

2.2. Patient samples

Leukemia cells were obtained from AML patients before chemotherapy. A summary of AML patient samples used in this study is shown in Supplementary Table 1. One sample with high expression of EVI1, PT11 cells, were cultured in RPMI 1640 supplemented with 10% FCS and 1 ng/mL GM-CSF. This study was approved by the Institutional Review Board of the Faculty of Medicine, University of Miyazaki. Informed consent was obtained from all donors in accordance with the Declaration of Helsinki.

Other materials and methods are given in the Supplementary data.

3. Results

3.1. Ang1 expression is high in EVI1^{high} leukemia cells

In our previous study, the expression level of Ang1 was found to be markedly decreased in embryonic HSCs derived from EVI1-deficient mice [11]. To investigate the correlation between the gene expression levels of EVI1 and Ang1 in leukemia cells, we performed semi-quantitative RT-PCR for Ang1 using four EVI1^{high} leukemia cell lines (UCSD/AML1, HNT34, Kasumi-3, and MOLM1), five EVI1^{low} leukemia cell lines (HEL, HL60, U937, K562, and NH), five leukemia cell samples from EVI1^{high} AML patients and eight leukemia cell samples from EVI1^{low} AML patients. As shown in Fig. 1A and C, the expression of Ang1 was up-regulated in the EVI1^{high} leukemia cell lines and AML cells from EVI1^{high} patients as compared with the EVI1^{low} leukemia cell lines and AML cells from EVI1^{low} patients, respectively. The high expression of Ang1 in leukemia cell lines and patient samples with EVI1^{high} expression was also confirmed by quantitative real-time RT-PCR (Fig. 1B and D).

3.2. Ang1 gene expression is regulated by EVI1 in EVI1^{high} leukemia cells

To investigate whether the expression of Ang1 is regulated by EVI1 in EVI1^{high} leukemia cells, we knocked down EVI1 expression in UCSD/AML1 cell line by introducing a small hairpin RNA (shRNA) against EVI1 (or shNega as a nonsilencing control). Examination of the levels of Ang1 by semi-quantitative and quantitative RT-PCR revealed that the level of Ang1 mRNA was significantly lower in the AML1/shEVI1 cell lines than in the control cell lines (Fig. 2A and B). The same experiment was performed using primary leukemic cells derived from a patient with inv(3)-bearing AML (PT11). We obtained very similar results in that the expression of Ang1 was down-regulated in the primary AML cells expressing shEVI1 (Fig. 2C and D). These results indicate that the expression of Ang1 is dependent on EVI1 expression in EVI1^{high} leukemia cells.

3.3. Ang1 suppresses cell cycle progression in EVI1^{high} leukemia cells

To investigate whether Ang1 is involved in cell cycle regulation in EVI1^{high} leukemia cells, we established UCSD/AML1 cell lines